PHYSICAL REVIEW D **86,** 036001 (2012)

Chiral symmetry breaking/restoration in a dyonic vacuum

Edward Shuryak[1,2] and Tin Sulejmanpasic[1,3]

[1]*Department of Physics and Astronomy, Stony Brook University, Stony Brook, New York 11794, USA*
[2]*Kavli Institute of Theoretical Physics, University of California at Santa Barbara*
[3]*Institut für Theoretische Physik, Universiät Regensburg, D-93040 Regensburg, Germany*

(Received 23 February 2012; published 8 August 2012)

We discuss the topological phenomena in the QCD-like theories with a variable number of fundamental fermions N_f, focusing on the temperatures at or above the critical value T_c of chiral symmetry restoration. The nonzero average of the Polyakov line, or holonomy, splits instantons into (anti)self-dual dyons, and we study both the bosonic and fermionic interactions between them. The high temperature phase is a dilute gas of ''molecules'' made of $2N_c$ dyons, neutral in topological, electric, and magnetic charges. At intermediate temperatures the diluteness of the ''molecular gas'' reaches some critical level at which chiral symmetry gets restored: we comment on why it is different for the fundamental and adjoint fermions. At high density the ensemble is a strongly coupled liquid with crystal-like short range order: we speculate about its possible structure at small and large N_f. We finally show that certain lattice observations are in agreement with the proposed model, and suggest a number of further lattice tests.

DOI: 10.1103/PhysRevD.86.036001 PACS numbers: 11.30.Rd, 11.15.Ha

I. INTRODUCTION

A. Qualitative overview

Here we outline the qualitative findings that emerged during the course of this study, and provide the answers to some of the questions that followed from it. A history of the works and ideas that lead us to these answers will be provided in the next subsection.

It is perhaps necessary to explain what we mean by the ''dyonic vacuum.'' Dyons in general are objects possessing both electric and magnetic charges. However, the term is used in two very different contexts. Historically, the first one is the ''particle dyons'' (Julia-Zee), the excitations of 't Hooft-Polyakov monopoles, well known in the Georgi-Glashow model and many supersymmetric theories: we will *not* discuss those in this work. The second type is the ''self-dual dyons,'' which appear as constituents of the instantons. Rather than being particlelike *excitations* of the vacuum, as the monopoles and the first type of dyons are, they are part of the vacuum itself, describing certain topologically nontrivial configurations of the gauge fields. Not being particles, they do not have momenta or kinetic energies: they appear in the QCD partition function integrated over their collective variables. Color orientations and sizes of instantons are re-interpreted as the positions of the dyons. In the case of the $SU(2)$ color group, there are two dyons per instanton, commonly called the M type and the L (or twisted) type, (see Table I). For a review of instanton dyons see [1,2] and references therein.

Here are some physical questions we will discuss:

(i) What are the interactions between dyons, especially between the self-dual and anti–self-dual ones?
(ii) How do fermions contribute to the interaction between dyons?
(iii) What is the qualitative picture of the dyon statistical ensemble, as a function of three key parameters, the temperature T and the number of fundamental N_f or adjoint N_a quarks in the theory? In particular, why does the chiral transition moves to a stronger coupling?
(iv) In the high-T limit, gauge field topology was described as a dilute gas of instanton–anti-instanton molecules [3]. How are these objects modified for the case of the nonzero holonomy in the language of dyons?
(v) What is the Dirac eigenvalue spectra for different dyonic ensembles? At which condition does chiral symmetry breaking take place?
(vi) Can one explain the dependence of the chiral phase transition on N_f and/or N_a?
(vii) Can one evaluate the ''gaps'' in the Dirac eigenspectra which are developed at $T > T_c$ using the dyonic ensemble?
(viii) At $T > T_c$, using the quenched ensemble of gauge fields, it has been found on the lattice that the chiral properties crucially depend on the particular periodicity conditions for the fermions. In particular, the *periodic* ones do not show a chiral restoration transition, unlike the (physical) *anti-periodic* fermions. How can one understand these observations?
(ix) Why does the chiral transition strongly depend on the color representation of the fermions, such as the fundamental or adjoint ones?

The reader perhaps noticed that this list of questions includes neither a discussion of the holonomy potential nor other questions related to confinement (such as e.g. in [4]). We think that any assessment of the back reaction of the dyons on the holonomy can only be done after a more

TABLE I. The charges and the mass (in units of $8\pi^2/g^2T$) for 4 $SU(2)$ dyons.

Name	E	M	Mass
M	+	+	v
$\bar{M}$	+	−	v
L	−	−	$2\pi T - v$
$\bar{L}$	−	+	$2\pi T - v$

quantitative theory of their ensemble emerges. The purpose of this paper is to take a step toward developing such a theory. Thus, here we will consider the holonomy $\langle P(T)\rangle$ as given, e.g. by the lattice data.

Now we outline our observations. It is convenient to discuss them by defining three regimes, from high to low T. We will call them:

(i) High $T \gg T_c$ case, the regime of a dilute molecular gas

(ii) Intermediate regime, $T = (1..2)T_c$, interacting molecular gas

(iii) Dense regime, $T < T_c$, dyons form a strongly coupled plasma, in their liquid phase

Here are further explanatory comments on each of those:

(i) High temperature implies weak coupling and thus the semiclassical treatment of instantons/dyons is applicable. Since these objects have nonzero electric fields, subject to the perturbative Debye screening, their density at high T is strongly suppressed. In a resulting dilute regime, the ensemble forms a "molecular gas" of objects that have zero topological, electric, and magnetic charges. The average Polyakov line in this regime is close to 1, i.e. the "Higgs vacuum expectation value (VEV)" $v \approx 0$, so all M-type dyons are light, while "heavy" L, $\bar{L}$ dyons have nearly all the action of instantons/anti-instantons. Instanton–anti-instanton molecules were described in [3] and subsequent works: and in the high-T limit we expect to be close to those results.

Fermionic zero modes of the instantons are shared by their constituents in a way that depends on the type of fermion of the theory. Physical antiperiodic fermions have zero mode of the (twisted) L, $\bar{L}$ dyons. As the number of fundamental fermions N_f in the theory increases, they bind them into tight $L\bar{L}$ "clusters," which play a role of the nucleus of these molecules. Consequently, the chiral symmetry is unbroken and the lowest Dirac eigenstates "at the gap" correspond to independent $L\bar{L}$ clusters, see Fig. 1.

The standard Abelian electric charges of both L and $\bar{L}$ are equal to -1, so the clusters has the charge -2. (The molecule thus looks like anti-He, with M, $\bar{M}$ as "positrons" around it.) A particular sign of a charge does not violate C parity, of course, because the Abelian fields are color projected to the color direction of the holonomy field $\sim \mathrm{Tr}(F_{\mu\nu}A_4)$, or more precisely $\sim \mathrm{Tr}F_{\mu\nu}L$, where L is the Polyakov loop. Since both non-Abelian fields in it are C odd, the product is C even. These signs are just a matter of the definitions used in the field.

Lattice practitioners sometimes use the so-called "valence" or nondynamical quarks (not included in the partition function) as a tool for the analysis of the gauge configurations. Those may have arbitrary properties and periodicity conditions. The "valence quarks" *periodic* over the Matsubara time have completely different zero modes and interact with the lighter M-type dyons. Those are also more weakly correlated than the L-type ones. The difference in their Dirac eigenspectra will be important tool in testing the structure of the dyonic vacuum.

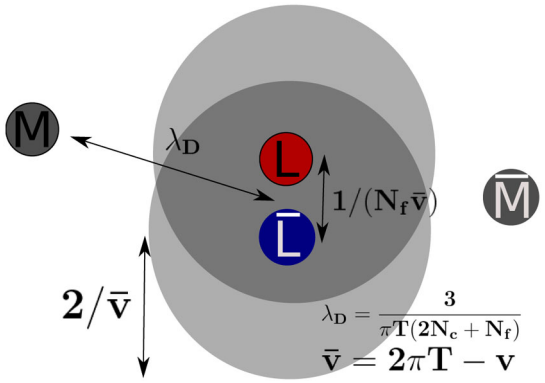

FIG. 1 (color online). The schematic picture of the dyonic molecule, for 2 colors and large N_f.

(ii) As T is lowered, the effective electric coupling $\alpha_s(T) = g^2(T)/4\pi$ grows and eventually becomes large $\alpha_s = O(1)$. A quite specific point introduced in [5] is the so-called "E/M equilibrium point," at which $\alpha_s(T) = 1$. Because of the Dirac condition for electric and magnetic couplings

$$\alpha_s \alpha_{\text{magnetic}} = \text{integer} \tag{1}$$

at this point, with integer being 1, the magnetic alpha is also 1. It has been argued and confirmed on the lattice that at this point magnetic excitations—monopoles—become about as numerous as the usual electric excitations, quarks, and gluons. In gluodynamics (no fermions, $N_f = 0$) this happens at $T \approx 1.4T_c$: how this depends on the presence of fermions remains to be studied.

Below T_c, the confinement forces the density of the electric objects (quarks and gluons) to be zero, while the magnetic (monopoles) retain the finite density. Only at $T \to 0$ does it disappear as well, with only the magnetic condensate remaining. Consequently, the electric Debye mass disappears

at $T < T_c$, while the magnetic screening mass remains finite. This implies that the electric screening of instantons at high T is substituted by a magnetic screening at $T < T_c$. As argued in [6], the latter creates a factor in the density of the instanton $\sim \exp(-\rho^2 \times \text{const})$, where ρ is the instanton radius and the constant, due to *magnetic* screening, has a nonzero value even at $T \to 0$ and is related to *Bose-condensed* magnetic monopoles. In certain dual models this constant was further related to the QCD string tension const $= 2\pi\sigma$ [6]. The expression describes well the lattice data on instanton size distribution and also explains why in the QCD instanton ensemble remains relatively dilute even at $T = 0$. It would be very interesting to see if any of that remains to be true at large N_f.

Near T_c magnetic screening should be induced mostly by the scattering of *non*-Bose-condensed monopoles. To our knowledge no study of the effect has ever been done, and we also defer it to future studies.

The interrelation between the ''particle monopoles'' (inducing confinement by their BEC) and the instanton dyons (inducing chiral symmetry breaking as we discuss below) is of course an intriguing open problem. On the level of gauge configurations themselves or their zero modes one finds no direct relation between them. However, at the level of the effective 't Hooft Lagrangian an intriguing relation has been found by Poppitz and Unsal [7] in the $N = 2$ compactified super Yang-Mills case. It appears at the level of the partition functions, one being the sum of the particle-dyon excitations and another the sum over the periodic instanton-dyon semiclassical solutions. Such relation clearly deserves further study and generalizations.

While any perturbative expressions/intuition is obviously not to be trusted in the regime of $\alpha_s(T) \approx 1$, the lattice simulations treat this region consistently. Furthermore, as we will detail below, in QCD-like theories with many fermions the plasma phase extends to even stronger coupling of $\alpha_s \sim 3$ or so. Perhaps the dual-–magnetic-formulation of such theories can be used in this case, as the magnetic coupling is getting weak $\alpha_{\text{magnetic}} \sim 1/3$.

Our paper, as many others, rely on the robustness of the topological effects under deformations, even if the amplitude of those is not small. Furthermore, topology is related (by index theorems) to fermionic zero modes. A ''collectivized'' set of such fermionic states contributes significantly to the quark condensate, pions and strongly influence the structure of the lowest hadronic states and correlation functions [8]. In contrast to the papers discussed in that review, we now approach this problem ''from above,'' starting from the hot symmetric phase at $T > T_c$ and follow the evolution of the topological quark states, from localized to delocalized ones as the transition temperature is approached.

Lattice data tell us that in the temperature interval $(2..1)T_c$ the average Polyakov line $\langle P(T) \rangle$ changes from ≈ 1 to ≈ 0. The holonomy changes from $\nu = 0$ to $\nu = 1/2$, at which point the masses (i.e. actions) of the L, M-type dyons become comparable. We also know that at the latter point confinement phenomenon takes place.

(iii) We can only qualitatively discuss the dense regime near and below T_c, as the interaction between the dyons becomes very strong. We try to approach the problem from the perspective of the strongly coupled classical plasma.

For large N_f the basic objects include the $L\bar{L}$ clusters which, we will argue, strongly repel each other. Therefore, the optimal correlations in such a medium would be similar to other systems that experience strong repulsive forces, such as closely packed liquids. While the global order is absent, locally those are strongly correlated, with the type of correlations being similar to those in certain best-packed crystals.

For zero N_f the dominant forces are Coulomb-like and corrections to them are in a form of the determinant proposed by Diakonov and collaborators, as well as the screening ones. If so, we suggest dyonic crystals resembling salt: cubic with alternating L, M dyons.

(Needless to say, we do not think that the solid is actually reached; it is well known that strongly correlated liquid have short-range correlations that are the same as their fully orderedcrystalline-form. While the ''dyonic crystals'' discussed provide examples of configurations in which the interaction is minimized, thermal fluctuations do kill the long range order, making it a liquid. Perhaps it is worth mentioning that the main parameter in the Boltzmann exponents, the mean ratio of the interaction potential per particle to T, also called Γ, needs to be $\Gamma > \Gamma_c \sim O(100)$ for solidification. In the dyon problem discussed this is not so, as $\Gamma \sim O(10) \ll \Gamma_c$).

Let us now focus on the main observable to be discussed, the Dirac eigenvalue spectrum and possible chiral symmetry breaking. With the increasing number of fundamental fermions N_f in the theory, they induce stronger correlations and reduce the size of the $\bar{L}L$ ''clusters.'' If one wants to follow the lines of constant quark condensate, e.g. the chiral restoration line, one has to increase the density of the clusters accordingly. This can only be achieved by a shift to stronger coupling.

As the dyon masses and interactions are $\sim 1/g^2$, they become lighter and less interacting. (Needless to say, their fermionic zero modes and related interaction must still be there, for topological reasons: they do not depend on the coupling.) The (dimensionless) density of dyons continue to grow to the situation in which the inter-dyon distances become comparable to the $L\bar{L}$ molecule size.

The adjoint fermions are very different from the fundamental ones. Some of them remain "massless" (in the sense of the "holonomy mass") after adjoint Higgsing, and this drastically changes the dependence of the "hopping amplitudes" on the distance, from exponential to power-like. The chiral symmetry is unbroken above such T when not only heavy L but also light M dyons have zero modes. This puts the chiral phase transition at much weaker coupling (higher T).

B. From instantons to dyons

The discovery of the instanton solution [9] has created a great deal of literature, including electroweak physics of baryon charge nonconservation as well as the famous exact results for various supersymmetric theories. Obviously we cannot review this amount of literature here.

In the context of the QCD-like theories, the predecessor of this paper is the so-called instanton liquid models, for a review see [8]. Its main point was to account for the so-called 't Hooft interactions to arbitrary order, by including the fermionic determinant in certain approximation in numerically simulated statistical ensembles. The calculated point-to-point correlation functions have reproduced many lattice results related to chiral $SU(N_f)$ and $U(1)$ symmetries. Chiral restoration can be viewed as the disappearance of the nontrivial solution to the so-called gap equation. Alternatively, it was explained [3] as a consequence of a structural phase transition in the instanton ensemble, from a random plasma at low T into a gas of strongly correlated $\bar{I}I$ instanton–anti-instanton pairs. The pairing mechanism is due to the fermion exchange, thus it gets stronger as N_f grows.

Let us recall its basic ideas, which will be used below. In the basis spanned by the zero modes of individual instantons/anti-instantons, one can write the Dirac operator as

$$i\not{D} = \begin{pmatrix} 0 & T_{IA} \\ T_{AI} & 0 \end{pmatrix}, \tag{2}$$

where we have introduced the overlap submatrix T_{IA}

$$T_{IA} = \int d^4x \psi^\dagger_{0,I}(x - z_I) i\not{D} \psi_{0,A}(x - z_A), \tag{3}$$

where I, A are indices which run over all instantons and anti-instantons in the configuration. Here, $\psi_{0,I}$ is the fermionic zero mode. The individual matrix elements have the meaning of a hopping amplitude for a quark from one pseudoparticle to another, and the determinant of this matrix is nothing else but the sum over the loop diagrams in which quarks visit each instanton once. Note that two ψs have opposite chirality, so if i = instanton then j = anti-instanton or v.v. The fermionic determinant is approximated by $|\det(T_{ij})|^2$. The low-T ensemble is a dense liquid that breaks chiral symmetry, but at high T (small size in τ direction) it breaks into "$\bar{I}I$ molecules" and chiral symmetry gets restored. The actual calculation was a simulation of the ensemble with the weight containing $|\det(T_{ij})|^2$, which was then used for the evaluation of the Dirac spectra and hadronic correlation functions. At high T, the approximate factorization of the Dirac matrix into independent 2×2 boxes (for separate clusters) explains the deformation of the Dirac eigenvalue spectra and disappearance of near-zero eigenvalues and the existence and the magnitude of the spectral gap G.

We will now extend these ideas to the case of the nonzero holonomy, the gauge-invariant closed loop integral over the $x^4 = \tau$ circle $\int_0^{1/T} d\tau A_4$. Its exponent, the so-called Polyakov line, averaged over the statistical ensemble of fields, has a nonzero value

$$\langle P \rangle = \left\langle \frac{1}{N_c} \mathrm{Tr}\, P \exp\left(i \int d\tau A_4^a t^a\right) \right\rangle \neq 0. \tag{4}$$

This calls for classical solutions that do not approach zero fields at spatial infinity but rather some constant value υ of the A_4^3 [in $SU(2)$]. We will also use dimensionless notations

$$\nu = \frac{\upsilon}{2\pi T}, \qquad \bar{\nu} = 1 - \nu. \tag{5}$$

Explicit solutions of such type [10,11] demonstrate that an instanton gets split into the N_c constituent dyons. The names and quantum numbers [for the simplest $SU(2)$ gauge group we will discuss in this work] cover all four possibilities for the electric and magnetic charges, see Table I. For $SU(N_c)$ in general there are $M_1, M_2 \ldots M_{Nc-1}$ static dyons with all diagonal charges and one "twisted" L dyon.

Let us indicate here the qualitative difference that the nonzero holonomy brings into this problem. The fundamental fermions in the "Higgsed" vacuum with a VEV of A_4 are "massive," with masses (in $SU(2)$) $m_f = \pm g\upsilon/2$. Therefore, the zero modes at large distances $r \to \infty$ decrease exponentially with the distance, unlike the power behavior typical for the zero holonomy case. These rapidly decreasing fermionic amplitudes are of course further enhanced by the number N_m of fermionic zero modes

$$e^{-V} \sim \det T \sim e^{-N_m m_f r}, \tag{6}$$

which creates strong linear confining potential for the corresponding dyons and thus produces small-size "clusters" of the size

$$\langle r \rangle \sim (N_m m_f)^{-1}. \quad (7)$$

The number of the modes is dependent on the fermion's color charge and the number of its copies. For the usual fundamental quarks $N_m = 2N_f$, as there is a zero mode for a quark and for an antiquark.

For the adjoint fermion $N_m = 2N_c N_a$. Furthermore, adjoint fermions that are diagonal with respect to the Polyakov line VEV remain "massless." The interaction between the dyons due to an exchange of the adjoint fermions has been discussed by Unsal [12]. The center of his proposal is a "bion," a cluster of $L\bar{M}$ dyons with the magnetic charge 2. Such bions can induce Polyakov-like confinement in the spatially compactified QCD [12].

C. Overview of lattice data on chiral symmetry restoration and deconfinement

1. The critical lines versus the number of fermions N_f, N_a

Let us start by reviewing some recent lattice results. Our version of the phase diagram uses the "critical lattice coupling"

$$\beta_c(T_c) = \frac{2N_c}{g^2(T_c)} \quad (8)$$

as a function of N_f or N_a. The "bare" coupling values in lattice works are defined at the lattice UV scale a. In order to make it lattice independent, we have evolved the scale from a by a factor of N_t (the number of points in the time direction) to the physical scale $N_t a = 1/T_c$ using the two-loop beta function. The near overlapping points in Fig. 2(a) are from different N_t simulations: their spread is a measure of the inaccuracy of the two-loop beta function used.

The open diamonds in Fig. 2(a) correspond to lattice data from Ref. [13]: they show the critical line of the chiral restoration (thin solid line). Above the line one finds the symmetric [quark-gluon plasma (QGP)] phase, below is the chirally broken (and confining) one. Moving downward on this figure means increasing the gauge coupling or decreasing the temperature. Thus, at $N_f \sim 10$ one may reach "the most strongly coupled QGP," which is by itself a very interesting phenomenon. Why is it happening?

(There are many other simulations reported in the lattice literature, of course: we decided not to put those on this plot because the rather different actions used produce rather random spreading of the couplings, confusing the observation).

The situation at $N_f = 12$ is special. Reference [14] argued that the chiral symmetry remains unbroken. A more recent paper [15] studied the region of even stronger coupling $6/g^2 \sim 1$, and perhaps clarified the observation. Two distinct phase transitions are observed, with the chiral condensate disappearing at stronger coupling (the closed diamond in Fig. 2(a)] than the confinement (the closed box). Thus, a novel intermediate phase in between is confining but chirally symmetric. An understanding of its precise nature remains a challenge, although such examples are known in supersymmetric theories.

The same authors [15] also concluded that for $N_f = 12$ those transitions are also separated by a bulk transition from a weaker coupling domain, in which there seem to exist a conformal (infrared fixed point) behavior. If so, the two phase transitions must be below (on the other side of)

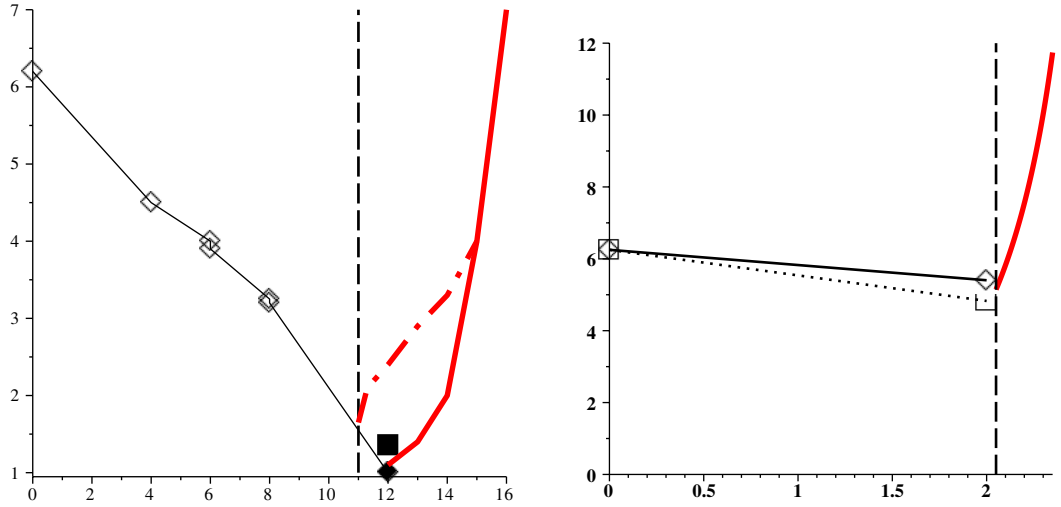

FIG. 2 (color online). The critical lines for chiral restoration (solid line and diamonds) and deconfinement (dotted line and boxes) of the $N_c = 3$ gauge theory. We plot the critical lattice coupling $\beta_c(T_c) = 6/g_c^2(T_c)$ versus the number of fundamental quarks N_f in (a) or a number of adjoint quarks N_a in (b). Both paths of the infrared fixed point, calculated in the two-loop approximation, are shown by the thick (red) lines. The vertical dashed lines separate the "conformal window domain": its location is a guess. In Fig. (a) we also show, by the dash-dotted (red) line, our guess for the actual location of the fixed point. For the meaning of the data points see the text.

the true trajectory of the fixed point schematically shown by the (red) dash-dotted line. This line may deviate from the thick solid (red) line, showing a fixed point line using the two-loop beta function, because of the very strong coupling involved. The issue of where exactly the conformal window starts remains unresolved. We tentatively put the vertical dashed line separating it at $N_f = 11$ in the figure. This is not a prediction but just a guess, and should not be used in any way.

Changing the fundamental quarks into either (i) adjoint (triplet in $SU(2)$, octet in $SU(3)$) or (ii) symmetric rang-2-tensor (triplet in $SU(2)$, sextet in $SU(3)$) shifts the T_c of the chiral transition upwards. The theory with two adjoint fermions, $N_a = 2$, has been studied in detail, see Fig. 2(b) based on [16], but (to our knowledge) not for other values, notably $N_a = 1$. (Of course, introducing variable masses may allow to follow the lines continuously.) Two distinct transitions were found, but in the opposite order in the previous case of the fundamental fermions. So, between the solid and the dotted lines there exists the *deconfined but chirally broken* phase (a plasma of constituent quarks). Furthermore, while the difference between these two points may appear small on this plot, the actual T_c scales of the two transitions are different by about factor 8. (It is also noteworthy that these points are close to the conformal window perturbatively, or perhaps already inside it nonperturbatively. We tentatively put its boundary—the vertical dashed line—at $N_a > 2$: it is not a prediction. Its exact location needs to be found numerically in future works).

2. The magnitude of the chiral splittings versus N_f

For N_f up to at least 8, the low-T theories retain both confinement and chiral symmetry breaking, but the quantitative relation between them changes. Let us characterize it by the relative splittings between the chiral partners, such as vector-axial $\rho - A_1$ mesons or the nucleon and the lowest $1/2^-$ N^* resonance at $T = 0$

$$\Delta_{\rho A_1} = 2\frac{m_{A_1} - m_\rho}{m_{A_1} + m_\rho} \tag{9}$$

$$\Delta_{NN*} = 2\frac{m_{N*} - m_N}{m_{N*} + m_N}. \tag{10}$$

The N_f dependence of these ratios is interesting: in the interval $N_f = 0..3$ these chiral splittings are "large" near the experimental values (i.e. at $N_f \approx 2.5$)

$$\Delta^{\rm exp}_{\rho A_1} \approx 0.45 \qquad \Delta^{\rm exp}_{NN^*} \approx 0.55, \tag{11}$$

which are well reproduced on the lattice. Yet calculated for the $N_f = 4$ [17] and 8 [18] theories, one consistently finds about twice smaller values, and at $N_f = 12$ these splittings were not observed at all [14,18]. In view of the trend just discussed, as well as because of the two transition observed in [15], we expect the chiral and deconfinement lines to separate, perhaps already at $N_f > 4$ or so.

3. Sensitivity to the fermionic periodicity conditions

Introducing an arbitrary phase in the periodicity condition of the "valence quarks," one can switch the fermionic zero mode between the dyons: this has been demonstrated using artificial configurations for calorons, e.g. in [19]. There is significant literature covering efforts to understand the difference in lattice gauge configurations below and above T_c. A paper presenting interesting results on the Dirac eigenvalue spectrum in the $SU(3)$ quenched and unquenched ensembles is that by Bilgici *et al.* [20]. Its brief summary:

(i) at $T > T_c$ the Dirac spectrum has a well-determined *gap* G (no eigenvalues inside $\lambda < |G|$), growing approximately linearly

$$G \sim (T - T_c), \qquad T > T_c \tag{12}$$

in the quenched case, until at least about $2T_c$.

(ii) if arbitrary (twisted) boundary conditions are used for (valence) fermions, with a phase $\phi = 2\pi z$, they seem to be irrelevant below T_c but change the results drastically above it. $\langle\bar\psi\psi\rangle$, or the density of eigenvalues at zero, seem to have a simple dependence on the angle

$$|\langle\bar\psi\psi\rangle| \sim c_1(T) + c_2(T)\cos\phi \tag{13}$$

with only one harmonic and positive coefficients c_1, c_2. For the holonomy values shifted above T_c by $\pm 2\pi/3$ the phase of the cosine is shifted accordingly.

(iii) As a result, antiperiodic fermions $\cos\phi = -1$ have a density that touches zero at T_c and develops a gap, restoring chiral symmetry. The periodic fermions, with $\cos\phi = 1$, never do so and their $\langle\bar\psi\psi\rangle$ grow indefinitely above T_c.

4. Chiral restoration in different Polyakov phase sectors

The previous issue is strongly related to lattice observations that subensembles of quenched configurations at $T > T_c$ with *different Polyakov phases* show different spectra of the Dirac eigenvalues and chiral parameters. In $SU(3)$ there are two sets, one with $\langle P\rangle$ real and another with the phase $e^{\pm i2\pi/3}$. For example, Fig 1 of [21] shows that these two different subensembles not only have different eigenvalues but also drastically different "participation ratios" (a degree of mode localization on the lattice). This phenomenon gives us the opportunity to study more than one set of holonomies in one simulation.

5. The spectral gaps at $T > T_c$ versus the fermion periodicity conditions

The gap opening is clearly observed for antiperiodic fermions but not for periodic ones, see [20]. An explanation based on dyon-antidyon classical correlation at high T_c was offered in [22]. Similar studies based on quenched configurations have been extended to adjoint fermions in Ref. [23]. Like for fundamental quarks, the antiperiodic adjoint fermions show a clear gap opening above the chiral transition, while the periodic ones do not.

6. Identifying the topological objects via their fermionic zero modes

In configurations with say exact $Q = 1$ one can locate one exactly zero mode and see the location of the corresponding eigenvector is space-time. Using such lattice configurations Gattringer and Schaefer. [24] have observed that while the eigenvector does indeed locate a single "topological lump," its position and quantum number depend on the boundary phase and jump at certain values, resembling what happens with the different types of constituent dyons inside classical caloron solutions. Such techniques allow locating all kinds of dyons and potentially study their correlations/interactions.

At $T \sim T_c$, with massless fermions and restored chiral symmetry, all configurations with nonzero Q are absent, and the Dirac eigenvalues get gapped. What are the states "at the gap," with the *lowest* Dirac eigenvalues at $T > T_c$? As demonstrated in [25], those have *two* topological lumps, confirming the observation of the paired instanton–anti-instantons [3]. As we will argue below, in the language of dyons, these molecules are more complicated, with $2N_c$ dyons of all kinds and certain Abelian charge distribution. Therefore, now one should use this method again, to look at Abelian-projected charges, clarifying their structure further.

More recently, Bruckmann *et al.* [26] looked at the fermionic states at the chiral gap at 2.6 T_c for quenched $SU(2)$ gauge simulations. They have shown that the corresponding eigenstates are well localized and correspond to a strongly modified local value of the Polyakov line. They observe that the number of such objects vastly exceeds the density of the isolated topological charges deduced from topological susceptibility, ruling out an ideal instanton gas as their source. They also commented, at the end of the section on topology, that their data "do not exclude" configurations in which the topological charge cancels, like the instanton–anti-instanton molecules to be discussed.

II. DYON INTERACTIONS

A. Classical interaction

As is well known, classical interaction of the dyons *inside* one of the sectors—self-dual or anti–self-dual—are absent, as they are protected by the Bogomolny-Prasad-Sommerfeld bound. Although it is clear how this works from the explicit solutions [11,27], we will still discuss it in the dilute limit, as our starting point.

The question of Higgs topology and monopole interaction has been addressed in many articles (e.g. [28–30]). Recall that the usual Higgs field has to go to zero at the monopole center because there is no preferred direction of color there. However with our "Higgsing" by the Polyakov loop, which is an element of $SU(2)$, and its value at infinity [which defines an unbroken $U(1)$ direction], the Polyakov loop can be viewed as $L \in SU(2)/U(1) = S^2$ mapping. At points without definite color direction the Polyakov loop takes a value of $L(\vec{x}_0) = \pm 1$: thus, two types of dyons. Indeed, the effective "Higgs" field at the dyon's center it is going to zero for M type and to $A_4 = \pi\hat{\phi}\cdot\vec{\tau}$ for the twisted L dyon, where $\hat{\phi}$ is a unit color vector (see below).

For a caloron—the $L - M$ pair in $SU(2)$—one can see from quantum numbers that both the electric and magnetic charges are opposites, so they should both create attraction. Another long-distance force is Higgs mediated: because dyons of M and L types have different value of the A_4 at their centers this turns out to be repulsive. Furthermore, it *exactly cancels* the attractive Coulomb forces, as required by Bogomolny-Prasad-Sommerfeld.

Now we consider dyon-antidyon pairs, starting with $M\bar{M}$ (which do not have a temporal twist, i.e. dyons completely static in time). We take them at a large distance $d \gg 1/v$ compared to the size of their cores. Inside some ball around the dyon (antidyon) of radius r_0 such that $1/v \ll r_0 \ll d$ the field strength can be written as a small deviation from self-duality due to the other dyon, i.e. of the order $1/d$. Outside of these balls the "Higgs" field is given by $|A_4| = v - 1/r_1 - 1/r_2$, where $r_{1,2}$ are distances from the dyon and antidyon, so as to conform to the expected asymptotic formulas for dyon and antidyon (see e.g. [2]).

For a single dyon the Higgs field can be written as

$$\vec{A}_4 = h(\boldsymbol{r})\hat{\phi}, \tag{14}$$

where $\hat{\phi} = \vec{A}_4/|A_4|$. Asymptotically $h(\boldsymbol{r}) = v - 1/r$. An ansatz that properly describes two dyons would have to obey the condition that asymptotically $|\vec{A}_4| \approx v - 1/r_1 - 1/r_2$. However, the color direction is a gauge choice that can be chosen arbitrarily at each point. Insisting that the Higgs points are in one color direction at some large sphere (gauge combing), one then has to introduce Dirac strings, as the gauge transformation cannot be made single valued. We do not specify this gauge choice, as we only deal with the action, which is gauge invariant.

That being said, we expect that the influence of the other dyon will change the h function by introducing an additive Coulomb term near the core of the first dyon, i.e. if $r_1 \ll r_2$, we have

$$H(\boldsymbol{r}_1, \boldsymbol{r}_2) \approx (h(r_1) - 1/r_2)\hat{\phi}, \tag{15}$$

where r_1 and r_2 are the distances from monopoles to the point of observation. An analogous relation holds when $r_2 \ll r_1$.

Now we determine the action of the system of two dyons, writing the action as an integral over three regions

$$S = \frac{\beta}{2}\left(\int_1 \mathrm{Tr}(F^2)d^3x + \int_2 \mathrm{Tr}(F^2)d^3x + \int_{\text{outside}} \mathrm{Tr}(F^2)d^3x\right), \tag{16}$$

where 1 and 2 denote the regions around the dyon and antidyon, respectively. Inside these regions we assume self-duality (anti–self-duality) up to some small correction of the order of $1/d$ inside the cores, i.e. $D_i A_4 = \mp\frac{1}{2}\epsilon_{ijk}F^{jk} + f_i$, where f_i is the field strength deviation from self-duality induced by the other (anti)dyon and is of order $f = o(1/d)$.

$$\begin{aligned} S_1 &= \beta\int_1 d^3x\left(\mathrm{Tr}(D_iA_4)\epsilon_{ijk}F^{jk}) + \frac{1}{2}\,\mathrm{Tr}f_i^2\right) \\ &\approx \beta\int_1 d^3x\partial_i(A_4B^i) + o(1/d^2) \\ &= 4\pi\left(\upsilon - \frac{1}{r_0} - \frac{1}{d}\right) + o(1/d^2), \end{aligned} \tag{17}$$

where the integration is over a ball of radius r_0 centered around the first dyon.

We pause to comment on a similar expression in the case when we have a single dyon. One can integrate on the surface at infinity, which would just simply yield $4\pi\upsilon\beta$, i.e. the usual mass of a dyon. However, it is more instructive to divide the region of integration into a small ball of radius r_0 and the rest. The small ball is a total derivative and yields the contribution $4\pi(\upsilon - 1/r_0)\beta)$ to the action. Then we can write the action as

$$S_{\text{single dyon}} = 4\pi(\upsilon - 1/r_0)\beta + \beta\int_{\text{outside}} d^3x\frac{1}{2}(E^2 + B^2), \tag{18}$$

where we integrate over the volume outside the ball. However, in this region the fields are Abelian and behave in an expected way. We can write $E_i = \frac{q_e\hat{r}_i}{r^2}\hat{\phi}$ and $B_i = \frac{q_m\hat{r}_i}{r^2}\hat{\phi}$ and the outside integral is $4\pi/r_0$. The sum of the region inside and outside gives the expected result $4\pi\upsilon$.

Coming back to the case of two dyons, we include the region around the antidyon and get

$$\frac{1}{2}\,\mathrm{Tr}\int_{\text{cores}} d^3xF^2 = 8\pi\left(\upsilon - \frac{1}{r_0} - \frac{1}{d}\right), \tag{19}$$

showing how one dyon has been modified by the presence of the other one. Next we write the integral outside as the sum of electric and magnetic parts, i.e.

$$E_i = \frac{\hat{r}_1^i}{r_1^2} + \frac{\hat{r}_2^i}{r_2^2}, \tag{20}$$

$$B_i = \frac{\hat{r}_1^i}{r_1^2} - \frac{\hat{r}_2^i}{r_2^2}, \tag{21}$$

which, upon integration, gives the expected interaction $4\pi/d$ for the electric and $-4\pi/d$ for the magnetic, and they cancel. Also there are two self-energy terms which are given by $4\pi/r_0$ for electric and magnetic field separately, which cancel the $1/r_0$ contribution to the inside-the-sphere integration.

Notice that even though the electric and magnetic fields cancel outside the cores, the dyon-antidyon system still attracts, due to the modification of their mass by the presence of the other (anti)dyon. Thus, there exists a long-distance classical Higgs-based attraction for the $M\bar{M}$ pair.

One can equally well consider $L\bar{L}$ dyons with the twist, i.e. with core time dependence. The only modification is that then the contribution to the action of the core is given by $4\pi\bar{\upsilon}$, where $\bar{\upsilon} = 2\pi - \upsilon$. Also, for a purely self-dual sector, the interaction of the L and M dyon is seen to cancel. This result is well known from the original works [10,11], but here we see that since the Higgs asymptotic looks like $\upsilon - 1/r_M + 1/r_L$ (see [2]), the Higgs interaction is repulsive, which exactly *cancels* the attractive forces of the E and B field. Note also that due to this effect of "dyon mass renormalization" we expect that if the L dyon has a fermionic zero mode (which as we will see in the next subsection, depends on this holonomy), it is renormalized by the presence of the other M dyon. This was observed in the original papers by van Baal *et al.* and it followed from the exact zero mode expression: we just identify its physical origin.

B. Fermion-induced interactions

Fermionic interactions between dyons are central for this paper. They are induced by the presence of fermionic localized modes facilitated by the time-dependent twist in the gauge fields. The fermions introduce the fermionic determinant $\det\not{D}$ factor in the partition function. If both the dyon and antidyon are in isolation (at large distances), they have zero modes, which leads to vanishing determinant: thus, such configurations are excluded from the ensemble. Obviously, at finite r the modes are nonzero, and therefore the dyon-antidyon pair is attracted due to the fermions.

As was done for the instantons, one can look at the Dirac operator in the basis of localized zero modes of individual L and $\bar{L}$ dyons. The matrix element of the $\not{D}$ zero mode between two of those we denote as T_{IJ}, where the indices run through all dyon and antidyon zero modes. Since the Dirac operator in the chiral basis connects between the left and right fermions only, the diagonal elements are all zero, and only blocks $T_{I\bar{I}}$ and $T_{\bar{I}I}$ remain, where now I runs through the dyon zero modes only, and $\bar{I}$ through the antidyon zero modes only.

It is quite clear that in the case of a dyon-antidyon pair, since $\det T = -|T_{I\bar{I}}|^2$, we have that $V_{\rm eff} = -\ln(T_{L\bar{L}}(r_{L\bar{L}}))$. Since the matrix element is approximately $T_{L\bar{L}} \sim e^{-Mr/2}$, where M is the "holonomy mass" of the fermion, the resulting effective potential between dyons is linearly confining.

While in this paper we focus only on the zero modes of the fundamental quarks, we would like to mention some important works on the adjoint fermions, which naturally appear in the supersymmetric context. For periodic compactification, the corresponding index theorem is discussed in [31] (see also citations therein). an extensive discussion of the zero modes for the periodic and antiperiodic adjoint fermions can be found in [32].

1. Fermionic zero mode for arbitrary periodicity condition

As we mentioned in the Introduction, one should not confuse the "particle dyons" and "instanton" (or self-dual) dyons: while mathematically similar they are associated with quite different physics. The "particle" dyons are time-independent three-dimensional objects and their fermionic zero mode are three-dimensional normalizable and time independent. For the "instanton dyons" we need four-dimensional normalizable zero modes. Index theorems associate the latter ones with the topological charge Q of the four-dimensional theory: thus an instanton ($Q = 1$) consisting of N_c dyons possesses only one of those, which need to be somehow shared between the dyons. Another important technical difference is induced by the fact that in QCD-like theories the role of the Higgs boson is played by A_4 rather than scalars or pseudoscalars. As a result, the corresponding gamma matrix for Higgs is γ_0 (rather than 1 or γ_5): this makes the interaction with the Higgs chirally symmetric.

Let us generalize the fermionic (−) and bosonic (+) boundary conditions to a general "anyonic" phase

$$\psi(\beta) = \exp(-i\phi)\psi(0), \tag{22}$$

which should be satisfied by a normalizable solution of the Dirac equation

$$\not{D}\psi = 0, \tag{23}$$

containing the gauge field in the hedgehog ansatz [33]

$$A_i^a = \epsilon_{aij}\mathcal{A}\hat{r}^j, \tag{24}$$

$$A_4^a = \mathcal{H}\hat{r}^a. \tag{25}$$

We use the gamma matrix convention $\gamma^i = \sigma^2 \otimes \sigma^i$, $\gamma^4 = \sigma^1 \otimes 1$, so that $\gamma_5 = \gamma^1\gamma^2\gamma^3\gamma^4 = \sigma^3 \otimes 1$, and do the calculation for the right spinor component. The Dirac equation then reads as

$$(\sigma^\mu)_{\alpha\beta}(D_\mu)_{AB}(\psi_R)^B_\beta = 0, \tag{26}$$

where we explicitly wrote the Dirac indices α, β and color indices A, B, and where $\sigma^\mu = (1, i\sigma^i)$. Now we use the form [34,35]

$$\psi^A_\alpha = \alpha(r)\epsilon_{A\alpha} + \beta(r)[(\hat{\boldsymbol{r}}\cdot\boldsymbol{\sigma})\epsilon]_{A\alpha}. \tag{27}$$

We may choose to consider the matrix

$$\eta_{A\alpha} = -\psi^A_\beta\epsilon_{\beta\alpha} \tag{28}$$

as being in the ansatz

$$\eta = \alpha_1(r)1 + \alpha_2(r)\hat{\boldsymbol{r}}\cdot\boldsymbol{\sigma}. \tag{29}$$

A color matrix τ acts on this object from the left, and the spin matrix σ from the right, with an extra minus sign, i.e.

$$\sigma\psi = \eta\epsilon\sigma^T = -\eta\sigma\epsilon. \tag{30}$$

The density of the fermions is defined as

$$\psi^{*A}{}_\alpha\psi^A_\alpha = \mathrm{Tr}(\eta^\dagger\eta). \tag{31}$$

We now plug the ansatz into (26) and obtain the following two equations:

$$\alpha_1'(r) + \frac{\mathcal{H}+2\mathcal{A}}{2}\alpha_1 + \frac{\phi}{\beta}\alpha_2 = 0, \tag{32a}$$

$$\alpha_2'(r) + \left(\frac{\mathcal{H}-2\mathcal{A}}{2} + \frac{2}{r}\right)\alpha_2 + \frac{\phi}{\beta}\alpha_1 = 0, \tag{32b}$$

where we have assumed $\psi_R \propto e^{-i\phi t/\beta}$, i.e. that the Fermion has arbitrary periodicity condition in the imaginary time direction.

We solve Eq. (26) in the Appendix, and the result is shown in Fig. 3. However, here we can easily look at the asymptotic behavior of the solution, i.e. when $\mathcal{H}(r\to\infty) = v$ and $\mathcal{A}(r\to\infty) = 0$, then

$$\alpha_1'(r) + \frac{v}{2}\alpha_1(r) + \frac{\phi}{\beta}\alpha_2(r) = 0, \tag{33}$$

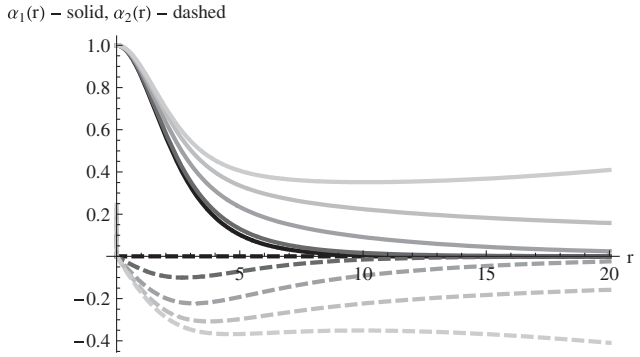

FIG. 3. The profile of (unnormalized) zero mode components $\alpha_{1,2}$ (the solid and the dashed curves) as a function of the distance from the dyon. We show four different values of $\phi = 0,\ 0.2v/\beta,\ 0.4v/\beta,\ 0.5v/\beta,\ 0.55v/\beta$. Note that the zero mode delocalizes at $\phi = 0.5v/\beta$.

$$\alpha_2'(r) + \frac{\upsilon}{2}\alpha_2(r) + \frac{\phi}{\beta}\alpha_1 = 0. \quad (34)$$

This equation is easily solvable. By taking the substitution $\alpha_\pm = \alpha_1 \pm \alpha_2$), we get

$$\alpha_\pm = e^{-((\upsilon/2)\pm(\phi/\beta))r}. \quad (35)$$

In order for the solution to be normalizable, we must have that both $\alpha_\pm$ vanish at infinity. This is only possible if $|\phi| < |\upsilon|\beta/2$.

2. The zero mode hopping

The formulas derived in the previous section explain why the zero mode "jumps" from one dyon to the other with the change in the periodicity condition of the fermions. However, there we assumed a static M-type dyon, which has the zero mode

$$\psi_M \sim e^{-((|\upsilon|/2)-|\phi|)r}, \quad (36)$$

where all dimensionful quantities are expressed in units of $\beta = 1/T$. Now it is quite clear that $\phi \in (-\upsilon/2, \upsilon/2)$ will preserve the normalizability of the solution. But for the phase in the interval $\upsilon/2 < \phi < \pi$, one can use the equation for the zero mode on the L dyon instead. To do so one must first go to the static gauge in which $\upsilon \to \bar{\upsilon} = 2\pi - \upsilon$, and then the zero mode has good asymptotic behavior

$$\psi_M \sim e^{-((|\bar{\upsilon}|/2)-|\phi|)r}. \quad (37)$$

Furthermore, because one has to apply a time-dependent gauge transformation to reinstate $A_4 \to \upsilon$ at infinity in the form $U = \exp(i\pi t\vec{\tau}\cdot\hat{r})$, the fermions (in the fundamental representation) gain the desired antiperiodicity. One can replace ϕ by $\bar{\phi} = \pi - \phi$, or

$$\psi_M \sim e^{-((|\bar{\upsilon}|/2)-|\bar{\phi}|)r}. \quad (38)$$

Now we insert $\bar{\upsilon} = 2\pi - \upsilon$ and $\bar{\phi} = \phi - \pi$, where ϕ and υ are the (true) holonomy and periodicity of the fermions. We assume $\phi \in (\upsilon/2, \pi)$, so that the exponential term can become

$$\frac{|\bar{\upsilon}|}{2} - |\bar{\phi}| = \pi - \frac{\upsilon}{2} - \pi + \phi = \phi - \frac{\upsilon}{2}, \quad (39)$$

and the fermion zero mode becomes normalizable for $\phi \in (\upsilon/2, \pi)$.

Finally, we explore the region $\phi \in (\pi, 2\pi - \upsilon/2)$. Then we argue that the zero mode on the L dyon is still normalizable. Indeed, the exponent now becomes

$$\frac{|\bar{\upsilon}|}{2} - |\bar{\phi}| = 2\pi - \frac{\upsilon}{2} - \phi \in (0, \pi - \upsilon/2). \quad (40)$$

Therefore,

$$\psi_M \sim e^{-(|\upsilon|/2-|\phi|)r} \quad -|\upsilon|/2 < \phi < |\upsilon|/2$$
$$\psi_L \sim \begin{cases} e^{-(|\phi|-|\upsilon|/2)r} & |\upsilon|/2 < \phi < \pi \\ e^{-(2\pi-|\upsilon|/2-|\phi|)r} & \pi < \phi < 2\pi - |\upsilon|/2 \end{cases}. \quad (41)$$

C. The fermionic interaction among the clusters

As it has already been mentioned above, on general grounds one expects the $L\bar{L}$ clusters to repel each other, as say atoms do, because of the Pauli principle. In this section we will show how it works using the first "non-diagonal" diagrams in which fermion exchange between such clusters takes place.

The fermion determinant will be of the form

$$\det\not{D} = |T_{1\bar{1}}|^2|T_{2\bar{2}}|^2\ldots|T_{N\bar{N}}|^2 - T_{1\bar{2}}T_{\bar{2}2}T_{2\bar{1}}T_{\bar{1}1}T_{3\bar{3}}\ldots T_{N\bar{N}}\ldots, \quad (42)$$

where $T_{1\bar{1}} = -T^*_{\bar{1}1}$. We can interpret the first term as a two-loop diagram, with the fermion hopping from one dyon to the antidyon and back, for each of the pairs $1\bar{1}$, $2\bar{2}$, etc. The second term is interpreted as a one-loop process, in which the fermion is hopping from 1 to $\bar{2}$ and then from $\bar{2}$ to 2 to $\bar{1}$ back to 1. The determinant is the sum of all such terms, with the appropriate minus sign to enforce the Fermi statistics. Note that the zero resulting from the cancellation between hose diagrams means that a dyon-antidyon pair will be repelled by another dyon-antidyon pair at certain distances.

It is simple to see that chiral symmetry is necessarily restored if the ensemble is made of dyonic pairs. Then the determinant is dominated by the near-diagonal matrix elements $T_{I\bar{I}}$, where indices I, $\bar{I}$ go over dyons and antidyons, respectively, which are the closest pairs, i.e. $T_{I\bar{J}} \ll T_{I\bar{I}}$, for $\bar{J} \neq \bar{I}$. Then the spectrum of the Dirac operator is exactly solvable and is given by $\lambda_I = \pm|T_{I,\bar{I}}|$. Therefore, very small eigenvalues will be given by the very small matrix elements $T_{I\bar{I}}$ of the dyonic pairs. This matrix element is small only if the respective dyons are very far away (much further than the range of the transition element, i.e. $1/\bar{\upsilon}$). But since the overall configuration is already weighted by the determinant to the power of the number of flavors N_f, these configurations are strongly suppressed, and the density of such eigenvalues goes to zero at small eigenvalues, implying that, by the Banks-Casher relation, chiral symmetry is restored.

An $2N \times 2N$ matrix of the form

$$M = \begin{pmatrix} 0 & A \\ -A^\dagger & 0 \end{pmatrix} \quad (43)$$

has a determinant equal to

$$\det M = |\det A|^2, \quad (44)$$

which is always positive.

Let us now consider the fermionic determinant in the basis of fermionic localized modes for 2 dyons and 2 antidyons, labeled with indices 1, 2 and $\bar{1}$, $\bar{2}$, respectively,

$$\det \not{D} = |T_{1\bar{1}}T_{2\bar{2}} - T_{1\bar{2}}T_{2\bar{1}}|^2. \tag{45}$$

As an example, consider a configuration of dyons and antidyons placed on a rectangle of dimensions $a \times b$. A little thought will immediately reveal that if we put them on a square such that as we go around we have $1\bar{1}2\bar{2}$, the determinant vanishes when $a = b$, or in other words, clusters $1 - \bar{1}$ and $2 - \bar{2}$ are mutually already infinitely repelling when $b = a$. However, we can make them come closer if we orient them on the rectangle as $1\bar{1}\,\bar{2}\,2$, i.e. dyons $1 - \bar{1}$ and $2 - \bar{2}$ form independent clusters with distance $r_{1\bar{1}} = r_{2\bar{2}} = a$ and $r_{1\bar{2}} = r_{2\bar{1}} = \sqrt{(a^2 + b^2)}$. Then the repulsion for small b/a will be

$$V_{\text{eff}} = -\ln(\det \not{D}) \sim -\log\left[T(a)T'(a)\frac{b^2}{a}\right], \tag{46}$$

where $T(r_{I\bar{I}}) = T_{I\bar{I}}$. Quite clearly the effective potential becomes infinite when $b \to 0$, making an effective repulsive core for the two dyonic clusters.

To discuss this further we introduce the diagrammatic interpretation of the determinant viewed as a sum over all fermionic loops. Let us view a determinant in some basis of local fermionic states. This need not (and in fact most certainly is not) be an eigenbasis of the Dirac operator. We denote the basis vectors as ψ_n, which are localized at $\boldsymbol{x}_n$. Since this basis is not an eigenbasis of the Dirac operator $\not{D}$, we have that

$$i\not{D}\psi_n = J_n, \tag{47}$$

where J_n is a spinor resulting from the action of the Dirac operator. However, we may view J_n as a source of our basis states, and interpret $\psi_n(y) = \int d^4y \Delta(x - y)J_n(y)$, where $\Delta(x - y)$ is the fermionic propagator. Then $\not{D}$ taken between two states $\psi_{m,n}$ will be

$$(i\not{D})_{mn} = \int d^4x d^4y J^\dagger_m(x)\Delta(x - y)J_n(y). \tag{48}$$

Therefore, we can view the matrix elements $T_{I\bar{I}}$ as hopping from one source to another.

The diagrammatic description of the determinant A in the upper-right quadrant is then (we assume $N_f = 1$ in what follows)

$\det A =$ 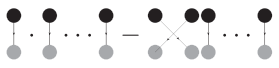 + (all possible perm)

where the black circle represents the dyon and gray circle the antidyon.

The complex conjugation can be viewed, instead of the fermion going from the dyon to antidyon, as the opposite propagation of an antifermion going from an antidyon to dyon. The pictorial representation of the determinant is

$\det \not{D} = |\det A|^2 = \det(A)\det(A^\dagger)$

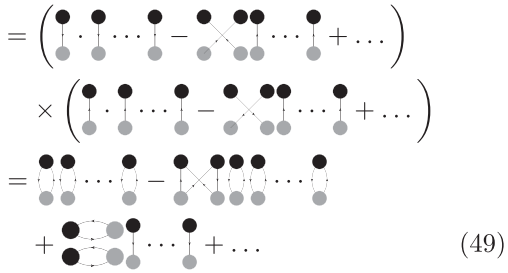 (49)

The interpretation of this expansion is then straightforward. The determinant can be interpreted as loop diagrams connecting the various dyons that carry a zero mode. It is quite evident from this diagrammatic expansion that every diagram of two loops will have a similar diagram with the opposite sign where the two loops join via a small channel (see Fig. 4).

Let us now think about how many pairs we can make from N dyons and N antidyons. After a bit of thought we can see that it is $N!$. All terms like that involve permuting in the above expression two positions of two (anti)dyons, and, because it requires two exchanges, the sign remains the same. The determinant will be integrated over the moduli space of the dyon-antidyon pairs, and so all of these kinds of permutations can be taken to be the same. Therefore, the first term will contribute with a factor of $N!$ to the determinant.

The second term is a bit more tricky. We proceed in the following way. Let us consider k 4-plets (a 2 dyon-antidyon pairs) which facilitate the one loop. The number of ways we can have one 4-plet is $(N(N-1))^2$, because we can pick two dyons in $N(N-1)$ ways, and the same for antidyons. For k such 4-plets have the expression

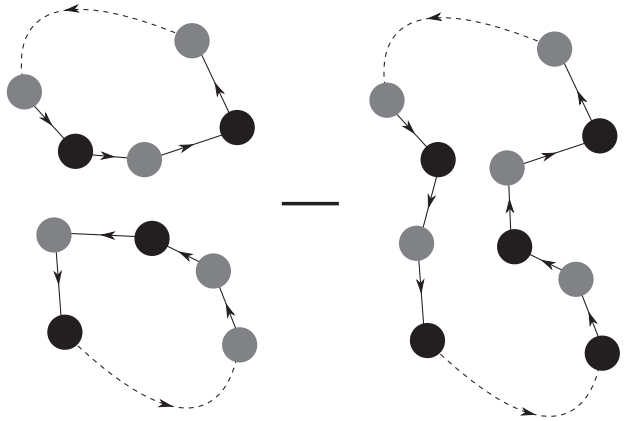

FIG. 4. A graphical interpretation of the weight in the background of the dyons. Note that the relative minus sign will always induce repulsion between the dyon and the antidyon in a dyon-antidyon pair.

$$N_{k-4\text{ plets}} = \frac{[N(N-1)(N-2)\dots(N-2k+1)]^2}{2^k k!}, \quad (50)$$

where the $k!$ factor is present to compensate for all possible interchanges of all k 4-plets. The rest of the dyons and antidyons can be made into pairs, and since there are $N-2k$ leftover (anti)dyons we can do this in $(N-2k)!$ ways. Combining this with the above factor we get

$$N^k_{4-\text{plets}} = \frac{N!^2}{2^k(N-2k)!k!}. \quad (51)$$

Now we consider the integrals over such matrix elements. Generally we will have that for the arrangement of pairs the integral over the moduli space (assuming flat moduli space metric—an assumption justified only in the dilute phase) will be given by

$$N!\left(c_0\frac{V}{m^3}\right)^N, \quad (52)$$

where c_0 is a constant that depends on a particular form of the matrix element $T_{I\bar{I}}$. In other words, we have written the integral $\int(T(r))^2 d^3r = c_0/m^3$, making it explicit that the effective volume of the integration measure is given by $1/m^3$, i.e. integrating over pairs will introduce a volume given by the range of their matrix elements $T_{L\bar{L}} \sim e^{-mr}$, and an overall volume corresponding to the integration over the center of mass of each pair. Notice that we also put in the factor $N!$, which is an overall degeneracy of the integral.

In the case of k 4-plets and $N-2k$ pairs, we have

$$\frac{N!^2}{2^k(N-2k)!k!}\left(c_1\frac{V}{m^9}\right)^k\left(c_0\frac{V}{m^3}\right)^{N-2k}. \quad (53)$$

The constant c_1 appears in the quadrupole integral over a loop that includes 4 (anti)dyons (2 dyons and 2 antidyons). The effective volume is now $1/m^9$, with a single, overall, volume factor. Therefore, the partition function can be approximated as

$$Z \approx 1/(N!)\left(c_0\frac{V}{m^3}\right)^N \sum_{k=0}^{N/2}\frac{(-1)^k N!}{2^k(N-2k)!k!}\left(\frac{c_1 n}{c_0^2 m^3 N}\right)^k, \quad (54)$$

where we have divided everything by$(N!)^2$ due to the indistinguishability of dyons and antidyons, and $n = N/V$ is dyon density. Rewriting

$$Z \approx 1/(N!)\left(c_0\frac{V}{m^3}\right)^N \sum_{k=0}^{N/2}\frac{(-1)^k N!}{(N-2k)!k!}\left(\frac{A}{N}\right)^k, \quad (55)$$

where the factor

$$A = (c1/2c0^2)n/m^3. \quad (56)$$

The coefficient $c1/c0^2$ is just a numerical factor, and it depends on how fast the matrix element falls off with distance, but it does not depend on an overall coefficient in front of the transition element.

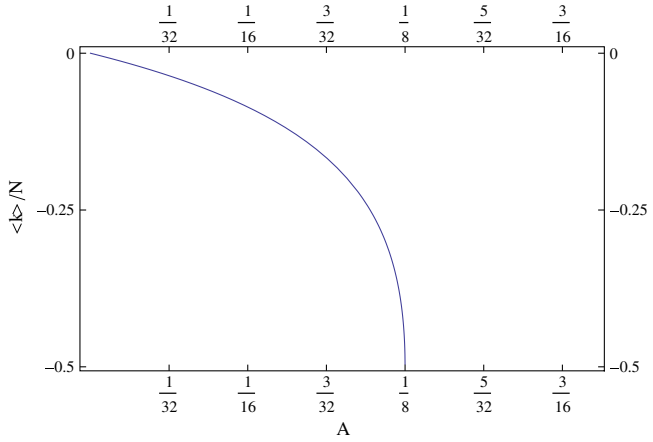

FIG. 5 (color online). $\langle k\rangle/N$ as a function of parameter A defined in (56).

The sum above can be computed by using the identity

$$H_N(x) = \sum_k^{N/2}(-1)^k\frac{N!}{k!(N-2k)!}(2x)^{N-2k}.$$

Then the partition function becomes

$$Z \approx 1/(N!)N^{N/2}\left(\frac{c_0\sqrt{A}}{nm^3}\right)^N H_N\left(\frac{1}{2}\sqrt{\frac{N}{A}}\right). \quad (57)$$

The approximation can only be valid if A is small; therefore, $1/A$ is large. We can employ an asymptotic form of a Hermite polynomial for large N in the following form [36]:

$$e^{-x^2/2}H_N(x) \approx, \quad (58)$$

$$\approx \frac{2^{N/2-3/4}\sqrt{N!}}{(\pi N)^{1/4}\sqrt{\sinh\phi}}e^{(N/2+1/4)(2\phi-\sinh 2\phi)} \quad (59)$$

for $x = \sqrt{2N+1}\cosh\phi$. Another asymptotic series assuming $x = \sqrt{2N+1}\cos\phi$ leads to oscillatory asymptotics, which is clearly a good indicator that our approximation of just including 4-plet diagrams is invalidated, and that higher order diagrams become important. For such an estimate the chiral symmetry will be restored for $A < 1/8$, or $n/m^3 < c_0^2/2c_1$, where n is the density of one species of dyons.

Finally, going back to (54) for a moment, we see that if we look for the quantity $\langle k\rangle = A\partial(\ln Z)/\partial A$, each coefficient will have a factor of k in front. (Note that this is *not* an average number of 4-plets: each configuration arbitrarily has many 4-plets, 6-plets, etc.). In Fig. 5 we show $\langle k\rangle/N$ as a function of parameter A. Notice the abrupt change as we approach the critical value $A = 1/8$, which we take as an indication of chiral symmetry breaking.

D. Bosonic one-loop interactions and electric screening

The basic physics of the electric screening can be explained most simply following the original derivation by one of us [37] (in the Coulomb gauge). If some object possessing a nonzero A_4 is immersed into a quark-gluon plasma, those quanta from the heat bath are scattered on it. The simplest diagram comes from the quartic term in the gauge Lagrangian, $\sim g^2 A_m^2 A_4^2$, which couples the heat bath gluons directly to the square of A_4, but there are also other diagrams contributing to the forward scattering amplitude. The result was the expression for the QCD Debye mass [38]

$$M_D^2 = g^2 T^2 (N_c/3 + N_f/6) \tag{60}$$

for massless quarks and gluons: incorporation of their effective masses is straightforward.

The next relevant paper is by Pisarski and Yaffe (PY) [39] who calculated the one-loop action of the calorons (the finite-T instantons). Its main part is the following correction to the instanton action:

$$\delta S_{\rm PY} = \frac{2\pi^2 \rho^2}{g^2} M_D^2, \tag{61}$$

where ρ is the instanton radius. The first factor in this expression comes from the (four-dimensional) dipole moment of the instanton, and the second from the forward scattering amplitude of the thermal plasma quanta on it (for the derivation see [40]). This term is only present in the plasma phase, at $T > T_c$, as only in this case there exist thermal quarks and gluons undergoing this scattering.

Going forward to calorons at nonzero holonomy, a corresponding one-loop effective action has been computed by Diakonov, Gromov, Petrov and Slizovskiy (DGPS) [4]. The caloron is now a superposition of the M and L dyons, separated by distance r_{ML}, and the basic expression from which the effect comes is the following integral:

$$\langle A_4^2 \rangle \sim \int d^3 r \left(\frac{1}{r_L} - \frac{1}{r_M} \right)^2 = 4\pi r_{ML} + \ldots, \tag{62}$$

where r_L, r_M are distances from the dyon centers to the observation point $\vec{r}$. (The dots stand for corrections due to a finite dyon size: the Coulombic A_4 is true only at large distance. Note also that at large r the integral converges because the integrand is $\sim r_{LM}^2/r^4$. This term comes again from the quartic term in the action, in which two gauge potentials are the A_4 of the instanton and two others belong to the thermal gluons).

Thus, the electric screening effectively generates the confinement of two dyons, with a potential linearly depending on the LM separation:

$$V_{\rm scr}^{LM} = r_{LM} \frac{2\pi M_D^2}{T g^2}. \tag{63}$$

At the zero holonomy this result matches the PY answer because of the "instanton size relation"

$$\pi \rho^2 T = r_{ML} \tag{64}$$

which, so to say, relates the four-dimensional dipole of the instanton to the three-dimensional dipole of the dyon pair. The second factor is still the same thermal integral producing T^2. One obvious effect of fermions is that a generalization of the DGPS result to theory with the generalized Debye factor as in (60). As a result, the electric screening effect ensures LM "binding" into a finite-size object with the (inverse) size

$$\langle r_{ML} \rangle^{-1} \sim T(N_c/3 + N_f/6). \tag{65}$$

Note also, that for $L\bar{L}$ or $M\bar{M}$ pairs with the *same* electric charge, there will be a plus in the integral (62) above and thus the effect becomes repulsive and the integral diverges: it needs to be regulated by some opposite charges. For molecules consisting of all 4 $(L, M, \bar{L}, \bar{M})$ dyons, to be discussed shortly, the screening potential is

$$V_{\rm scr} = \frac{M_D^2}{2Tg^2} \langle A_4^2 \rangle |_{LM\bar{L}\bar{M}} \tag{66}$$

in which the A_4 now contains all 4 Coulomb contributions. This integral is of course convergent because of the total zero charge of the molecule.

Let us give an example of the electric multi-dyon screening potential created in this case. We will later see that the direct fermionic interaction binds $L\bar{L}$ pairs stronger than the LM interaction. Therefore, for simplicity one can ignore the $L\bar{L}$ cluster size and put them at the same point, the origin. Another simplification appears if one puts M, $\bar{M}$, and $L\bar{L}$ on one line. The integral (62) changes to

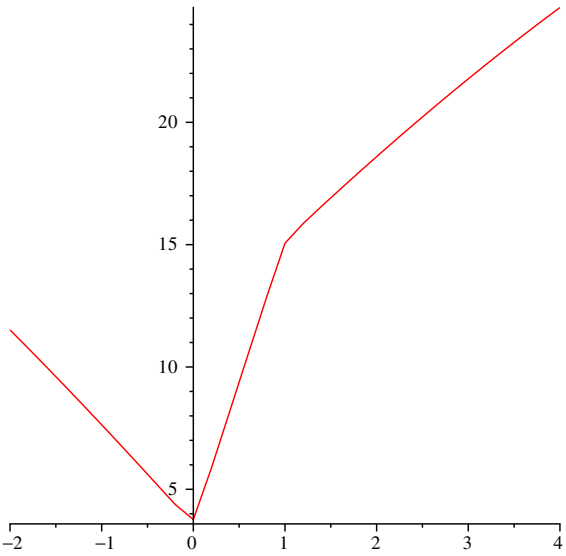

FIG. 6 (color online). The integral (67) proportional to the potential for the M (or $\bar{M}$) dyon created by the electric screening as a function of its position. The charge -2 $L\bar{L}$ pair is assumed to be in the origin, and the companion dyon is at point 1.

$$\int d^3r\left(\frac{2}{r}-\frac{1}{r_M}-\frac{1}{r_{\bar{M}}}\right)^2. \quad (67)$$

The corresponding potential is shown in Fig. 6. As one can see, like for DGPS case, the potential consists of linear segments, but is now deformed away from the companion dyon. (Note, that it is not due to their Coulomb repulsion, which is also there but will be discussed in the next section).

III. STATISTICAL MECHANICS OF DYONS

A. Statistical mechanics of a single dyonic molecule

The partition function for an instanton–anti-instanton molecule can be recovered using known elements for each of the ingredients. Let us start with dimensional considerations, valid at high enough temperatures. If the fermions are all massless, the overall power of the T dependence of total molecular density can be determined from the known power of the $\Lambda_{\rm QCD}$ in the instanton–anti-instanton measures, namely,

$$n_{\rm mol}=\frac{\log Z_{\rm mol}}{V}\sim T^3\left(\frac{T}{\Lambda}\right)^{-(11N_c/3+4N_f/3)}. \quad (68)$$

Typically the power in the second factor is large and negative, so this density rapidly decreases with T. (It is so except near the boundary of the asymptotic freedom domain where that power is getting small: we will not discuss this region).

The translation from the language of the dyonic to the language of the instanton at the level of the moduli metric and partition function has been studied for the self-dual and anti–self-dual sectors by Diakonov *et al.* [4]. Their expression, in the $SU(2)$ case for pure gauge theory is

$$dZ_{LM}=d^3r_L d^3r_M T^6 2\pi C\left(\frac{8\pi^2}{g^2}\right)^4 \times\left(\frac{\Lambda_{\rm PV}e^{\gamma}_E}{4\pi T}\right)^{22/3}F_D(r_{LM})e^{-V_{\rm scr}(r_{LM})}, \quad (69)$$

where $r_{LM}=|\vec{r}_m-\vec{r}_M|$, is the numerical constant $C=1.0314\ldots$, and the scale parameter $\Lambda_{\rm PV}$ is for the Pauli-Villars regularization [41] The factor

$$F_D(r)=\left(1+\frac{\upsilon\bar{\upsilon}r}{2\pi T}\right)(1+\upsilon r)^{(4\upsilon/3\pi T)-1}(1+\bar{\upsilon}r)^{(4\bar{\upsilon}/3\pi T)-1}$$

is the correction appearing due to the nonzero holonomy. If the holonomy $\upsilon=0$ or antiholonomy $\bar{\upsilon}=0$, in the expression above $F_D=1$, it reduces to the well-known caloron measure, using the relation (64). In the limit of large dyon separation one may keep only the r terms: note that it then becomes flat and r independent as one would expect. The screening potential for LM pair is

$$V_{\rm scr}(r)=\frac{2\pi r}{\pi^2 T}\left[\pi T\left(1-\frac{1}{\sqrt{3}}\right)-\upsilon\right]\left[-\pi T\left(1-\frac{1}{\sqrt{3}}\right)+\bar{\upsilon}\right]. \quad (70)$$

We have excluded one more factor in the partition function of [4]

$$\exp\left(-V\frac{\upsilon^2\bar{\upsilon}^2}{12\pi^2T}\right), \quad (71)$$

which does not depend on the calorons/dyons and is just a one-loop contribution to the probability to have the holonomy υ in the ensemble: it certainly should not be repeated twice.

The same expression can be repeated for the for the $\bar{L}$, $\bar{M}$ pair, and then combined into the 4-particle partition function for a "molecule." Since, unlike [4], we are interested in the theories with fermions, we introduced extra factors that include that for zero modes as well as the nonzero mode part

$$dZ_{\rm mol}=dZ_{LM}dZ_{\bar{L}\bar{M}}\left[\frac{m^2+|T_{IA}(r_{L\bar{L}})|^2}{\Lambda^2}\right]^{N_f} \times C(N_f)\left(\frac{\pi^2 r_{LM}r_{\bar{L}\bar{M}}\Lambda^4}{T^2}\right)^{N_f/6}e^{-V_{\rm scr}-V_{L\bar{L}}} \quad (72)$$

As discussed in the preceding section, $V_{\rm screening}$ is defined by the 4-particle expression for A_4 integrated over the volume. If one of the particles is going to large distances, the expression reduces to a dipole and returns the linear confinement result, preventing "ionization" of a molecule.

The bracket in the power of $N_f/6$ comes from the nonzero mode part of the fermionic determinant calculated by 't Hooft. The power of Λ in it corresponds to correct beta function of the theory with N_f fermions, and is therefore fixed. Its dimension should be compensated by some parameters with the dimension of the distance, which in the case of a single instanton can only be its size ρ. At finite temperature instantons lose four-dimensional spherical symmetry and another dimensional parameter—T appears, as well as a nonzero holonomy υ. Lacking explicit evaluation of the nonzero mode determinant, we just used the instanton expression and the relation $\pi\rho^2T=r$ translating its size into the current language. At least for small-size instantons (small r) this should work. As a result, we get factors $r^{3N_f/2}$ in the measure, or a repulsive potential $\sim N_f\log(1/r)$ trying to dissolve the molecule. Recall however that it is only supposed to be true at small r, while at large r the one-loop electric screening effects generate an attractive potential linear in r which would prevent it from happening.

We have introduced here the fermion mass m in the Dirac operator, assuming it is the same for all flavors, for normalization reasons [42]. The term proportional to the masses is nothing else but a square of the independent instanton and anti-instantons, and since their normalization has already been determined by 't Hooft, the flavor-dependent normalization constant $C(N_f)$ can be determined for $\Lambda_{\rm PV}$.

If the fermion masses are set to zero, the fermions couple the instanton to the anti-instanton via the overlap matrix element and four integrals over the dyon positions produce three convergent integrals, while the one remaining

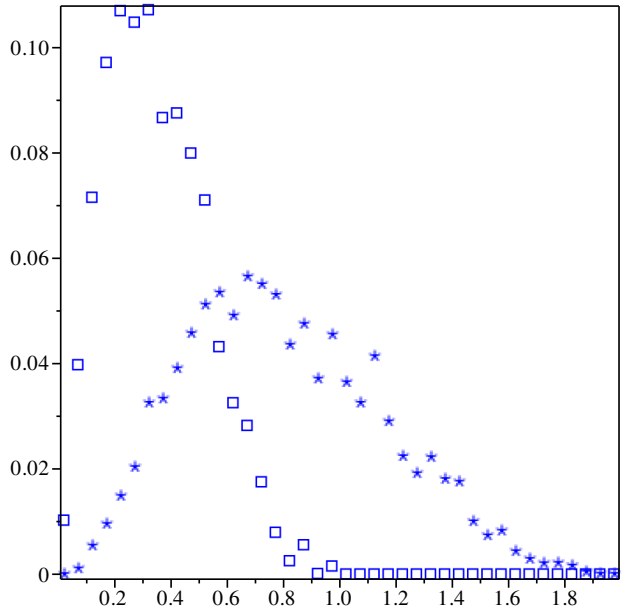

FIG. 7 (color online). Histograms of the distributions of the distance between the LM dyons (stars) and $L\bar{L}$ (boxes) dyons, for the $N_c = 2$, $N_f = 4$ molecule, in the units of the Matsubara time $1/T$. The fermionic mass is taken to be $m_f = T$ and the holonomy $\nu = 0.1$.

integral over the global position produces one factor of V, the box volume.

Even for the simplest case of $SU(2)$ color, when molecules contain 4 dyons, their position space is already 12-dimensional. Therefore, we used standard Metropolis algorithm to generate their statistical distributions. Figure 7 shows one typical example of the output: in it we compare the distances between the LM dyons (stars) with that of the $L\bar{L}$ (boxes). The latter are seen to be much tighter placed, forming a "nucleus" of the molecule.

B. Modelling the dyonic ensemble

1. Three molecular models

As a first step toward the understanding of dyonic ensembles and their role in chiral symmetry breaking/restoration, we have formulated some simplified models.

For calculation purposes it is convenient for these models to treat the density of the dyon as

$$n_d = n_L = n_M = n_{\bar{L}} = n_{\bar{M}} \tag{73}$$

(which is also the same as the density of the instanton $n_{\rm inst} + n_{\rm antiinstanton}$) as the basic dimensional quantity, providing the units of length $n_d^{-1/3}$. Using such length units we put $n_d = 1$ for awhile, and will be expressing other dimensional quantities in these units. We will be working with traditional periodic boxes of some size $L \times L \times L$, with L large, and thus put into such boxes $N_d = L^3$ dyons of each kind.

For each configuration of these models we then calculate the fermionic matrix T_{ij}, and calculate its eigenvalues. In this way we get part of the Dirac spectrum built on the subspace of the dyon zero modes. Since antiperiodic fermionic zero modes resign on L, $\bar{L}$ dyons only, the fermionic part of the measure ignores the M, $\bar{M}$ dyons. The matrix is thus of the size $2N_d \times 2N_d$. For reasons of opposite chirality, two quarters of the matrix, when both i, $j = L$ or $\bar{L}$ are zero, so fermionic hopping occurs only from a dyon and antidyon.

We assume the matrix element T_{ij}, which is given by

$$T_{ij} = c\frac{e^{-Mr_{ij}}}{\sqrt{1 + Mr_{ij}}}, \tag{74}$$

where one of the indices counts L dyons, and the other counts $\bar{L}$ dyons. The constant c will be left undetermined, whereas the mass M is given by

$$M = \bar{v}/2 = (2\pi - v)/2 \tag{75}$$

The form of the matrix element is not derived, but it is postulated as expected from the matrix element of the Dirac operator in the zero mode basis. We introduce a regulator at $r = 0$, so as to make smooth distributions. However, there will be an natural cutoff for how close the dyon and antidyon can get before they are part of a perturbative vacuum, which is already roughly the size of their cores $1/M = 2/\bar{v}$. Strictly speaking, the definition of the distance at which the dyon-antidyon pair is irrelevant is defined as the distance at which it no longer supports a localized fermionic mode.

We proceed by three models:

(i) The random gas model

(ii) The random molecular model

(iii) The reweighted molecular model

The simplest model is that of the "random gas model," in which all correlations between the dyons are ignored and they are placed randomly. The only parameter of the model is the fermion mass M entering the matrix T_{ij}, to be expressed in units of $n_d^{1/3}$. (In reality, both the density of the dyon and the holonomy, defining M, will be a function of the temperature T, but we prefer to study our models in their parameter space before mapping some of the results to lattice data, see below).

In Figs. 8 and 9 we show the results of such calculation. We use the box of the size 6^3 and thus 216 dyons of each kind, and a range of fermion masses as indicated in the figure caption. The characteristic feature of the "random gas model" is a large peak near eigenvalues $\lambda \approx 0$. Since the density of quasizero eigenvalues is proportional to the quark condensate (Casher-Banks theorem), we conclude that this model provides large or "enhanced" chiral symmetry breaking.

Our second model is the "random molecules model," in which we include pair correlations between L, $\bar{L}$ dyons. As we discussed above, we expect significant attraction

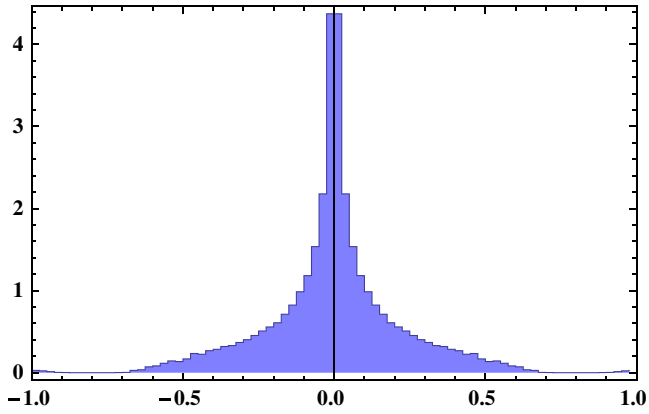

FIG. 8 (color online). The Dirac eigenvalue spectrum for the random dyon gas.

between those of classical (Higgs-related) origin, as well as the fermion-induced dyon-antidyon confinement. We focus here on the fermionic interaction. As the number of fermionic zero modes grows proportionally to the number of flavors N_f, we expect that at large enough N_f the molecule's mean size R_m decreases as $\sim 1/N_f$. We model the vacuum as being composed out of random molecules. The following distribution of the size of molecules is used:

$$D_{\rm mol}(r) = Nr^2\left(\frac{e^{-Mr}}{\sqrt{1+Mr}}\right)^{2N_f}, \tag{76}$$

where r^2 is due to the measure of the dyon-antidyon coordinates, and N is the normalization constant. The above form is inspired by a weight $(\det T_{ij})^{N_f}$, for a dilute molecule ensemble. The average molecular size will roughly be given by $R_m = 1/(N_f m)$.

At this stage we have ignored any interaction between the molecules, placing them randomly with random orientations.

The model has two parameters, the holonomy mass M and the number of flavors N_f. In Fig. 10 we show the Dirac spectrum for several values of N_f, as a function of M and in Fig. 11 the lowest eigenvalue and chiral condensate results. Note that here there is explicit dependence of the chiral condensate on the holonomy.

The third model is a modification of the second by reweighting the configurations with the determinant $(\det T_{ij})^{2N_f}/(\prod_i D_{\rm mol}(r_i i))$, where r_{ii} is the distance between its closest neighbors. The result is shown in Figs. 12 and 13.

2. Mapping the models to finite T QCD

Our three models were defined in such a way that each step has introduced one new parameter: with the density of the dyon, it brings the total number of parameters to four. Yet QCD-like theories with massless fermions have only two parameters, the temperature T and Λ. Thus, only a 2-parameter subspace of our (up to) 4-parameter model space can be compared to reality.

Now is the time to map those parameters. Like lattice practitioners do, it is thus natural to measure all dimensional quantities in units of T. The dimensionless density of the dyon n_d/T^3 is one of the key parameters. It has not yet been measured on the lattice, but it can be. While it is the same as the density of instantons, it is *not* given by the topological susceptibility $\chi(T)$, as neutral molecules contribute to the former but not the latter. Semiclassical theory tells us that the large T is asymptotically dependent on T, expression (68). For qualitative estimates one may use it normalized to its value at T_c. The factor in front of the power of T_c/T depends on the coupling, in a particular definition used by 't Hooft, and at the fermionic factors its value is $O(1)$ for physical QCD or $N_f = 2$, which one can use for absolute normalization.

The fermion mass $M/T \sim 1/N_f$ and thus, keeping the coupling fixed while increasing N_f, one finds that the cluster size is reducing and thus we are going into a regime of more dilute gas. However, if one wants to follow the line of "fixed eigenvalue spectrum" and/or fixed $\langle\bar\psi\psi\rangle$, one

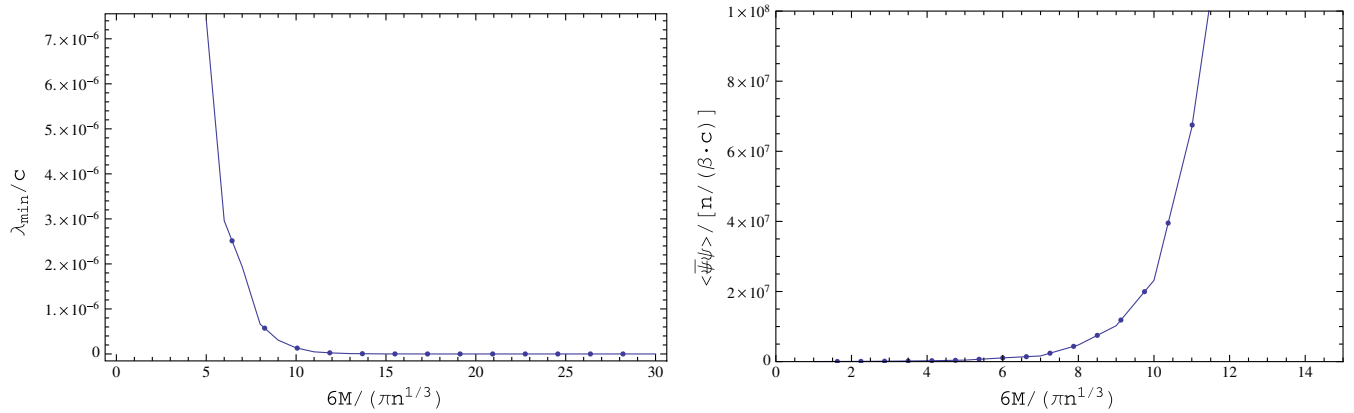

FIG. 9 (color online). The eigenvalue gap and the quark condensate for the random gas model, as a function of the "holonomy mass" M.

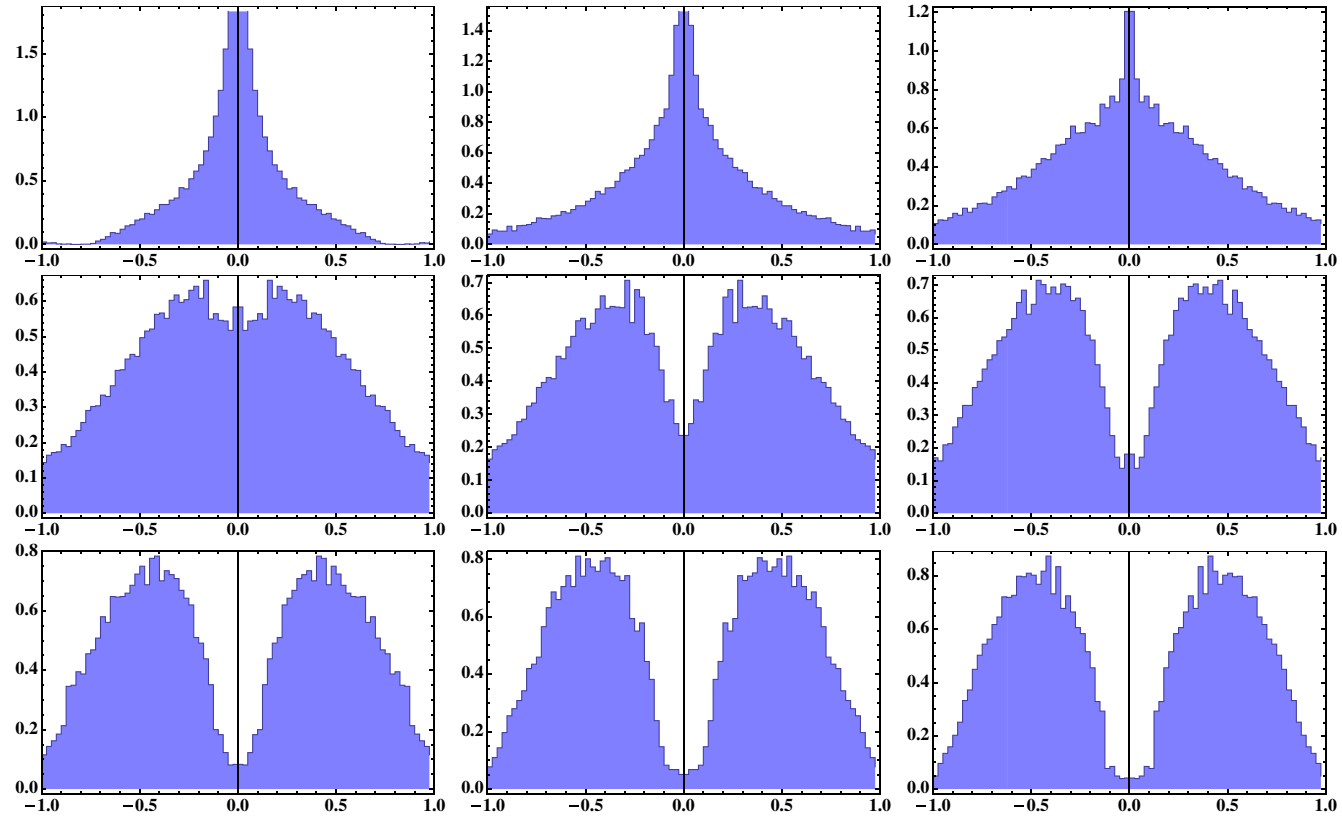

FIG. 10 (color online). The Dirac eigenvalue spectrum. The horizontal axis is the eigenvalue of the Dirac operator λ expressed in units of c defined in Eq. (74), and the vertical axis is the probability density dP/λ. The plots are for $N_f = 2$ and $M = (\pi/6 \ldots 9) \times \pi/6n^{1/3}$, where n is the density of L dyons. Note that the chiral symmetry is restored as a function of M, which is connected to the holonomy as $M = \bar{v}/2 = (2\pi - v)/2$.

needs to keep the same diluteness of the molecular model, or keep constant

$$R_m^3 n_d = \text{const}, \tag{77}$$

where $R_m \sim 1/(N_f M)$. Thus, the density of the dyon should grow as N_f^3, e.g. from $N_f = 2$ to 12 increase by a factor 216.

The only way it can be achieved is by a shift into the stronger coupling! A crude estimate ignoring the pre-exponent gives a shift of

$$\frac{8\pi^2}{g^2(T_c(N_f))} - \frac{8\pi^2}{g^2(T_c(N_f = 2))} = -3\ln(N_f/2). \tag{78}$$

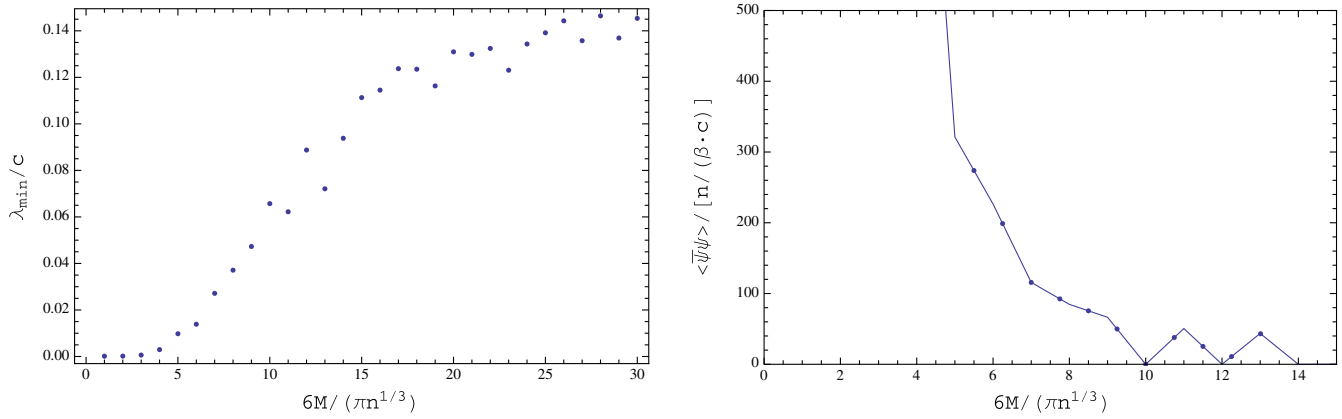

FIG. 11 (color online). The smallest eigenvalue and the chiral condensate for the random molecule model, as a function of the holonomy mass combined with the density of the dyon for $N_f = 2$.

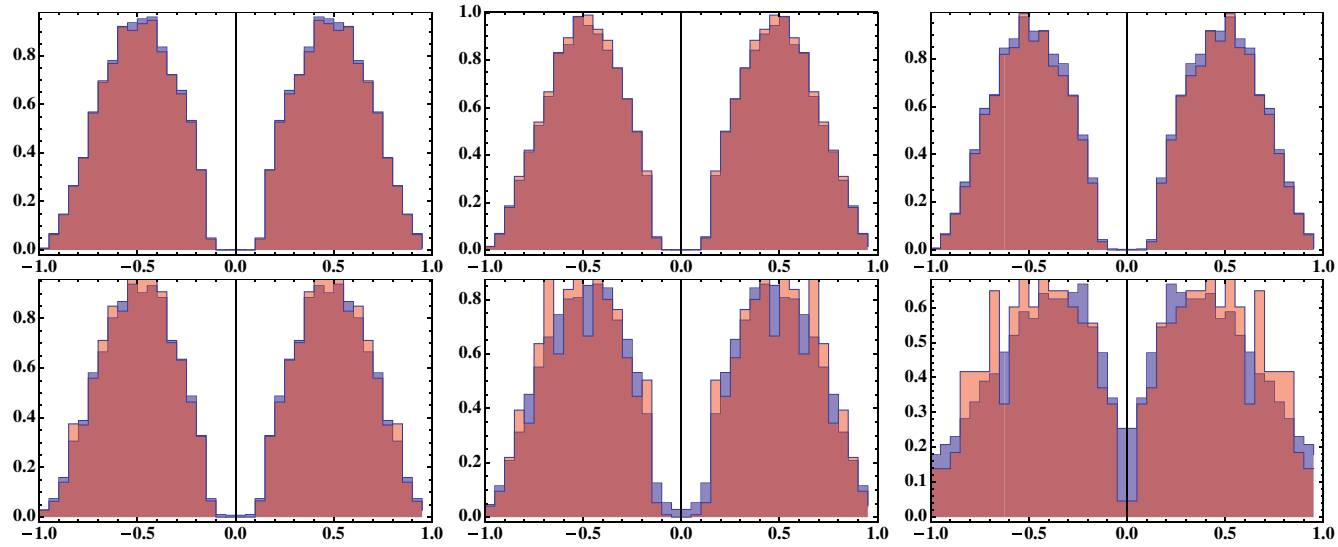

FIG. 12 (color online). The Dirac eigenvalue spectrum for a random molecule ensemble light (blue) and reweighted random molecule ensemble dark (red). The horizontal axis is the eigenvalue of the Dirac operator λ expressed in units of c defined in Eq. (74), and the vertical axis is the probability density dP/λ. The plots are for $N_f = 2$ and $M = (30, 25, 20, 15, 10, 5) \times \pi/6n^{1/3}$, where n is the density of the L dyons. The reweighting becomes unreliable in the last plot, and only one configuration dominates.

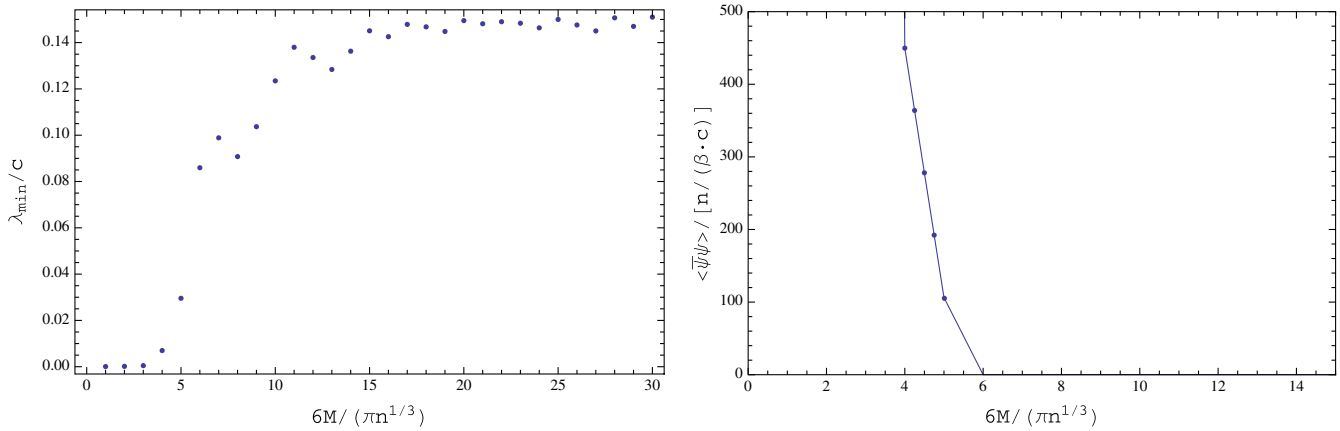

FIG. 13 (color online). The smallest eigenvalue and the chiral condensate for the reweighted random molecule model, as a function of the holonomy for $N_f = 2$ and $M = \pi/6 \ldots 30 \times \pi/6$. Note that reweighting becomes unreliable at around $M = 15 \times \pi/6$, and that we show this result only to demonstrate the trend that chiral symmetry persists to lower values of the holonomy mass M than for the nonreweighted case.

This qualitatively explains why the chiral restoration line $\langle \bar{\psi}\psi \rangle = 0$ derived in lattice studies (see Fig. 2) dramatically shifts into stronger coupling.

Unfortunately our attempts to do it quantitatively failed, for the following reason. The coupling g in the semiclassical expressions and on the lattice (such as in Fig. 2) are defined in different schemes, with the scales $\Lambda_{\bar{M}S}$ and $\Lambda_{\rm lat}$. Perturbatively they only differ by a calculable factor, but as their ratio happens to be large, this relation is not very useful in practice. For example, for QCD or $N_f = 3$ theory, the former is about 300 MeV and the latter about 5 MeV. The density of the instanton includes a huge factor

$$\exp\left(-\frac{8\pi^2}{g^2}\right) \sim (\Lambda_{\bar{M}S}/\Lambda_{lat})^{11Nc/3-2N_f/3} \sim 60^9. \quad (79)$$

Obviously, in view of such a huge factor, any small deviation from the two-loop beta function used would result in huge uncertainties which make any numerical comparison of the semiclassical expressions and lattice bare coupling meaningless.

The tests of this explanation however can still be made using lattice data. The most straightforward one would be to measure the density and size of the dyon molecule and see if the relation (77) holds. To do so one can, e.g., use

Dirac eigenstates in a certain interval of λ, which can identify a dyon-antidyon cluster.

3. Structure of strongly coupled "cluster liquid"

With a large number of fermions $L\bar{L}$ are strongly coupled into a charge -2 well localized objects, compensated by the negatively charged M and $\bar{M}$ dyons, which are more homogeneously distributed.

The $L\bar{L}$ "nuclei," with the fermions attracted to them, form mutually repulsive "atoms." The question is what arrangements those should have to get the lowest energy. One obvious idea is those with the best packing in three dimensions, namely, the face-center cubic or the hexagonal-close packing. Selecting between those one may follow the guidance given by ordinary atoms which are neutral and spherically symmetric by themselves. High-density solid He^4 is of the hexagonal-close-packing structure, and perhaps that would be the approximate local symmetry of our strongly correlated $L\bar{L}$ liquid. If so, each of them has 12 nearest neighbors, organized in two hexagons at two planes above and below the cluster.

While a large number of correlated neighbors reinforces the correlations, simple estimates show that the parameter Γ (the average interaction potential divided by T) does *not* reach the critical value needed for the ensemble to get solidified. Thus, with the parameter range at hand we expect a strongly coupled liquid, with smaller number of well-correlated neighbors but with their locations still correspond to those in the crystal. Explicit statistical simulations of it are possible, but are deferred for further studies.

C. Statistical mechanics driven by bosonic moduli space metric effects

Let us now discuss the opposite limit of $N_f = 0$, in which there is no $L\bar{L}$ clustering. Let us further imagine that for some reason one can decouple the two sectors, dyons and antidyons, and discuss what kind of a system would be created by "Diakonov's determinantal forces.". Assuming that the anti–self-dual sector does not exist, let us thus focus on the M, L sector. Since the electric and magnetic charges in it have the same sign, one may in this section simply call them $+$ and $-$ dyons.

At large distances the forces between them are Coulombic, and one may think that the local crystal correlations those generate is a simple cubic crystal of alternating charges, like, e.g. the usual salt NaCl. Any charge is thus strongly correlated with its 6 nearest neighbors.

Classical Coulombic systems are well known to be unstable against charges falling on each other. (Of course for real ions electron repulsion solves this issue, stabilizing the salts). We thus studied the following question: can the Diakonov's determinantal forces stabilize a cubic crystal?

We use the moduli space metric G_{ij} for the self-dual sector as suggested in [2] to calculate the effective potential of a crystal configuration of L and M dyons, with a lattice spacing a, for a displacement of a single dyon somewhere in a center. The effective potential is the log of the measure, $V_d = -\ln(\det G)$. For a purely Coulombic crystal, the crystal potential as a function of a displacement Δx has infinite Coulombic dips as displacement Δx approaches $\pm a$, which means that for purely Coulombic interactions the alternating charges will fall on each other. However the effective potential V_d contains repulsion and, as shown in 14, this leads to a pronounced minimum at $x = 0$ for sufficiently small lattice spacings a (high density). On closer inspection, however, there is always a small, but clear minimum. As expected, the Coulombic dips at $\pm a$ still persist. This divergence—corresponding to small-size instantons and the factor $1/\rho^5$ in the measure—is known to be removed by quantum fluctuations, which produce a stronger factor $\rho^{11Nc/3-2N_f/3}$. Thus, outside of classical approximation the problem is well defined.

On the other hand, as discussed in [2], it seems that from the point of view of the far field metric, the anti–self-dual sector behaves similarly to the self-dual one, and the interaction between L and $\bar{L}$ is similar to the interaction between L and L (i.e. repulsive), while that of L and $\bar{M}$ is attractive. Therefore, we have three possible structures depicted in Fig. 15:

For a nonzero number of quark flavors N_f fermions correlate the L and $\bar{L}$, then they will repel the other pairs, therefore making the hexagonal crystal, as we discussed

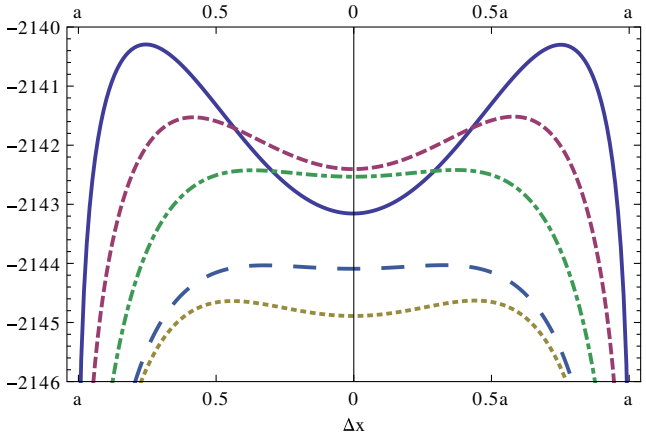

FIG. 14 (color online). The effective potential $V_d = -\ln(\det G)$, where G is the Diakonov determinant, as a function of the displacement Δx of a single dyon in the center of a cubic $6 \times 6 \times 6$ crystal, in the direction of the adjacent dyon. The graphs have been rescaled for better comparison as follows: (blue) solid $684V_d$, $a = 0.1$; (red) dash $818V_d$, $a = 0.25$; (brown) short dash $917V_d$, $a = .5$; (green) dash-dotted $967V_d$, $a = 0.75$; (blue) long dash $1000V_d$, $a = 1$. The units of Δx, a are the Matsubara time. Note that as the density of the dyon increases by a factor 10^3, this one-loop bosonic interaction creates a significant minimum at $\Delta X = 0$, stabilizing the cubic structure.

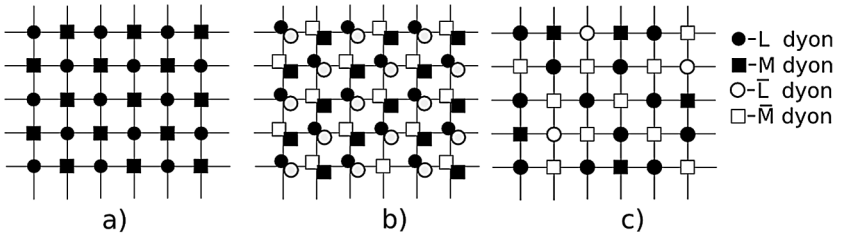

FIG. 15. Three possible crystal structures discussed in the text.

above. For zero N_f they can be either strongly correlated (b) or form an alternating crystal (c). Lattice practitioners often introduce the so-called valence quarks, which are not in the measure but are only used for a diagnostic purposes of the "quenched" ($N_f = 0$) theory. Dirac eigenvalue spectrum and chiral properties revealed by such studies can be computed and compared to the lattice data.

In a standard way we model the Dirac matrix by a "hopping" matrix (2, 3), with the matrix elements being some function of a distance between dyon-antidyon $f(r)$. We expect these functions to be exponential in distance $r = |\vec{r}|$ at large r and some constant we call $f(0)$ at small r.

In the first approximation we can consider only next-neighbor matrix elements, and use the cubic structure (b). Then we can write the upper-right (or the lower-left) part of the Dirac operator matrix, in the triple-index notations with n, m, l being positions in units of a along the three spatial coordinates in the cubic lattice

$$D^{n'm'l'}_{nml} = f(0)\delta^{n'}_{n}\delta^{m'}_{m}\delta^{l'}_{l} + f(a)(\delta^{n'+1}_{n}\delta^{m'}_{m}\delta^{l'}_{l} + \delta^{n'-1}_{n}\delta^{m'}_{m}\delta^{l'}_{l} + \delta^{n'}_{n}\delta^{m'+1}_{m}\delta^{l'}_{l} + \delta^{n'}_{n}\delta^{m'-1}_{m}\delta^{l'}_{l} + \delta^{n'}_{n}\delta^{m'}_{m}\delta^{l'+1}_{l} + \delta^{n'}_{n}\delta^{m'}_{m}\delta^{l'-1}_{l}). \quad (80)$$

Upon standard diagonalization by transformation to the dual lattice momentum states

$$|\boldsymbol{k}\rangle = \frac{1}{\sqrt{L^3}}\sum_{\boldsymbol{I}=(n,m,n)} e^{2\pi i \boldsymbol{I}\cdot\boldsymbol{k}/L}, \quad (81)$$

we obtain that the spectrum is given by

$$\nu(\vec{k}) = f(0) + f(a)(\cos k_1 + \cos(k_2) + \cos(k_3)), \quad (82)$$

where $k_{1,2,3}$ go from $(0, 2\pi)$, and the elementary number of states is given by standard $dN = Vd^3k/(2\pi)^3$. The density of states is

$$\frac{dN}{d\lambda} = V\int d^3k\,\delta(\lambda - \cos k_1 - \cos k_2 - \cos k_3), \quad (83)$$

where we have used the *shifted* eigenvalues

$$\lambda = (\nu - f(0))/f(a). \quad (84)$$

The spectrum can be integrated to yield

$$\frac{dN}{d\lambda} = \int dk_1 dk_2 \frac{1}{|\sin k_3(k_1, k_2)|}, \quad (85)$$

where $k_3 = \arccos(\lambda - \cos k_1 - \cos k_2)$, and the region of integration is such that $|\nu - \cos k_1 - \cos k_2| \le 1$. Numerical integration yields the curve shown in Fig. 16.

We see that the density of states form a band with a sharp boundary, it goes to zero at $|\lambda| > 3$. For scenario (b) this shape will appear in the spectrum centered around $\pm|f(0)|$, and, for vanishing $f(a)$, it will be delta function-like. Each of these morphs into the shape in Fig. 16 in a type (b) crystal as $f(a)$ increases. If they are separated by more than the width of the peak, the chiral symmetry is *not* broken. The condition for chiral symmetry breaking is therefore

$$\left|\frac{f(a)}{f(0)}\right| > \frac{1}{3}. \quad (86)$$

Alternatively, structure (c) can be motivated as follows. As mentioned earlier, the long range interactions between Ls and Ms, become the same regardless of them being dyons or antidyons. This means that the cubic crystal will have Ls and $\bar{L}$s located at the positions of the "+" ions and M and $\bar{M}$ at the positions of "−" ions. In this case, the spectrum of the Dirac operator is

$$\nu = 2f(a\sqrt{2})(\cos k_1 + \cos k_2 + \cos k_3 + \cos k_4), \quad (87)$$

where we have approximated that, on average, each L has 4 nearest $\bar{L}$s. Similarly as before we get that

$$\frac{dN}{d\nu}(\nu = 0) = 2f(a\sqrt{2})\int \frac{dk_1 dk_2 dk_3}{(2\pi)^4}\frac{1}{|\sin k_4|}, \quad (88)$$

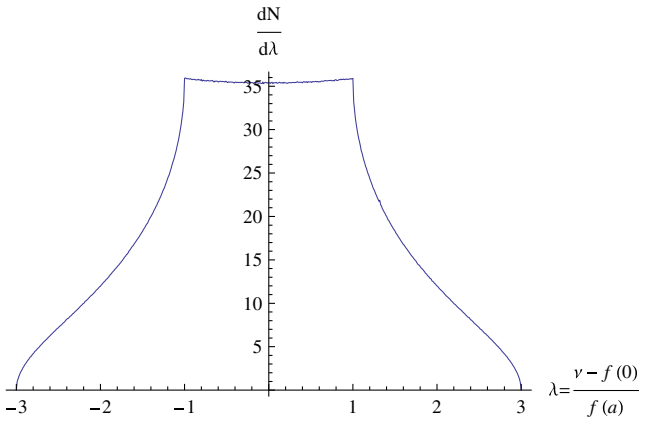

FIG. 16 (color online). The plot of the density of the states of the cubic lattice with the next-neighbor interactions.

where $k_4 = \arccos(\cos k_1 + \cos k_2 + \cos k_3)$, and $\cos k_1 + \cos k_2 + \cos k_3 \le 1$.

D. Note on confinement of the cubic crystal

Here we show that the Polyakov loop of a crystal configuration is indeed zero. We have that

$$\mathrm{tr}\, L(\boldsymbol{x}) = \mathrm{tr} e^{i((\upsilon/2)+V(\boldsymbol{x}))\tau_3} = 2\cos\left(\frac{\upsilon}{2} + V(\boldsymbol{x})\right), \quad (89)$$

where we used the gauge-combed gauge, and where $V(x)$ is some potential that goes to $-\upsilon/2$ at the position of the M and $\bar{M}$ dyons and to $-\upsilon/2 + \pi$ at the position of the L and $\bar{L}$ dyons. Using the identity that $\cos(\alpha + \beta) = \cos\alpha\cos\beta - \sin\alpha\sin\beta$, we have that

$$\mathrm{tr}\, L(\boldsymbol{x}) = 2\cos\frac{\upsilon}{2}\cos(V(\boldsymbol{x})) + 2\sin\frac{\upsilon}{2}\sin(V(\boldsymbol{x})). \quad (90)$$

The above expression has to be integrated over all possible crystal orientations and positions. This is equivalent, though, to integrating over $\boldsymbol{x}$ in the region of one crystal unit, i.e.

$$\langle \mathrm{tr} L(\boldsymbol{x})\rangle = 2\frac{1}{a^3}\int_{a^3} d^3x\left[2\cos\frac{\upsilon}{2}\cos(V(\boldsymbol{x})) + 2\sin\frac{\upsilon}{2}\sin(V(\boldsymbol{x}))\right] \quad (91)$$

However, setting $\upsilon = \pi$ (the maximally nontrivial holonomy), we see that the first term vanishes because $\cos(\pi/2) = 0$, and the second term vanishes because $V(\boldsymbol{x})$ is alternating between the L and M dyons in sign, and, since sin is an odd function, this term vanishes too. Therefore, the Polyakov loop averaged over crystal configurations vanishes, and it depends explicitly on the holonomy being nontrivial.

Finally, let us note that such "confinement in average" phenomenon has its predecessors, resembling a finite-density holographic model of densely packed baryons [43]. In it baryons are modeled by instantons, which also undergo a transition into a "dyon phase" in which they restore chiral symmetry in average.

IV. SUMMARY AND DISCUSSION

In this work we have done a qualitative study of the interactions of (anti)self-dual dyons, as well as some study of the statistical ensembles following from them. We emphasized in particular the importance of the *dyon-antidyon* interaction, both classical (bosonic) and fermion-induced ones, instead of the interactions inside the self-dual and anti–self-dual separate sectors. We specifically focused on the $SU(2)$ theory and the temperatures above and near the chiral restoration phase transition.

We have already summarized our overall findings from this study at the very beginning of the paper, so let us just outline the elements that we believe explain certain lattice observations. We will also emphasize what lattice practitioners can do to test our predictions further.

(i) Existence of the "topological molecules"
At high T the density of the instanton/dyon is small due to electric screening, the topological object must make molecules, neutral in terms of all three charges involved: topological, electric and magnetic. In the $SU(2)$ theory they contain all 4 types of dyons. We predict a peculiar distribution, with the nucleus of the $L\bar{L}$ cluster at the center, with M and $\bar{M}$ at the periphery, see Fig. 1. This effect is predicted to become more pronounced with the increasing number of quark flavors N_f. It is important to check it on the lattice, perhaps by identifying the fermionic states "at the gap" in ensembles with varying N_f. Its generalization to any number of colors is straightforward.

(ii) The critical line versus the fermion numbers N_f, N_a
Model simulations with such clusters, random or interacting with each other, predict certain distinct shapes of the Dirac eigenspectrum at small λ. We have in particular found at which diluteness of the "cluster gas" one gets a particular value of the chiral condensate, the chiral symmetry restoration or at a certain size of the gaps. These eigenvalue spectra and "lines of constant condensate" can be compared with the lattice ones, in order to see if chiral breaking does happen in the "molecular gas" regime, or at a denser regime.
The increasing number of fermions leads to stronger fermion-induced interactions, binding the $L\bar{L}$ pairs into tighter clusters. In terms of our molecular gas model, it becomes much more dilute, unless the overall density of the dyons is significantly increased. This can only be achieved by *going into a stronger coupling domain*, which reduces the dyon masses and interactions. That is why the critical lines in Fig. 2 go downward with increasing flavors. We have also explained why there is a qualitative difference between the fundamental and adjoint fermions. While the former have zero modes only with one (heavier) dyon $L\bar{L}$, the adjoint have zero modes for all dyons, including lighter M, $\bar{M}$ (for $SU(2)$). The latter are much less correlated, thus their chiral restoration temperature is much higher.

(iii) Chiral splittings of hadronic masses versus N_f
As this parameter is now becoming measurable on the lattice, with the progress in computer/lattice technology, it is perhaps time to map it more consistently, and also think again about the physics it reveals.
The rapid decrease of the chiral condensate scale around $N_f \sim 4$ has in fact been predicted

by the instanton liquid simulations [8] long ago. The reason for that has been a "dip" in the eigenvalue spectrum developed due to the molecule formation [44]. This very phenomenon is in fact central to our current study. What was not predicted in the 1990s was a significant shift to the stronger coupling and the drastic increase of the overall density of the instanton/dyon (in other words, a rapid decrease of the hadronic scale), which makes a very small quark condensate relevant. It would be important to study the transition to a "molecular" topological structure in lattice simulation.

The dependence of the quark condensate on the density of the molecules we found in our calculations is interesting. As seen in Fig. 10, at low density there is a minimum between two "molecular peaks," but at some diluteness there is the sudden appearance of a small peak inside this minimum. This implies a sudden jump in the quark condensate value, in a small interval of parameters. It is more pronounced than many crossover phase transitions, and thus we may call this phenomenon a phase transition in the dyonic ensemble, from an "atomic" to a molecular state, at $N_f > 3$. Using quark masses as interpolating parameters between $N_f = 3$, 4, 5, lattice practitioners can see if this change in Dirac spectrum is also occurring in lattice simulations as well.

(iv) Dependence of the Dirac eigenvalues on the holonomy value and phase

The nonzero holonomy provides Higgsing, the breaking of the color group, and thus it naturally explains the different fermionic holonomy "masses"' that appear in the T_{ij} hopping amplitudes. Since the $SU(2)$ gauge group was discussed earlier in this paper, let us discuss $SU(3)$ in a bit more detail, that is, the two $SU(3)$ options shown in Fig 1 of [21], namely, the real $\langle P\rangle$ sector as well as the one with the phase of P being $2\pi/3$. The generic holonomy in $SU(3)$ is described by 3 parameters μ_1, μ_2, μ_3 subject to one condition $(\mu_1 + \mu_2 + \mu_3 = 0(\mathrm{mod}(1))$. If one imposes an additional condition, such as the fixed phase of $\langle P\rangle$, there is only one free parameter left. If the phase is zero, $\langle P\rangle$ is real, and the 1-parameter family of possible holonomies is

$$\mu_1 = 0; \qquad \mu_2 = 1/2 - \delta; \qquad \mu_3 = 1/2 - \delta. \tag{92}$$

If the phase is $2\pi/3$, this solution is simply rotated additively to

$$\mu_1 = 1/3; \qquad \mu_2 = 1/3 + 1/2 - \delta; \qquad \mu_3 = 1/3 + 1/2 - \delta. \tag{93}$$

The masses of the monopoles are determined by the differences, which are the same in both cases,

$$\nu_1 = \nu_3 = 1/2 + \delta, \qquad \nu_2 = 2\delta, \tag{94}$$

since for the gluonic observable the two sectors are identical by the Z_{N_c} symmetry.

However the fundamental fermions notice the difference, as their masses are given by μ_i, not ν_i. Furthermore, which dyon gets the zero mode depends on the phase parameter z in the fermionic periodicity condition: the rule is that it is the one in which the ν sector z resides on the circle. The antiperiodic fermions ($z = 1/2$) pick up the second type of dyon $\nu_2 = 2\delta$ in the real sector and the first one $\nu_1 = 1/2 + \delta$ in the one with the $2\pi/3$ phase. The lowest mass of the fermion is $2\pi T\delta$ in the former case, while in the complex ones it is $(2\pi T) \times \min(1/6, 1/3 - \delta)$.

Of course, in the lattice subsector with the fixed phase, the modulus still has some average and the distribution, determined by the effective potential of $\langle P\rangle$ at a given T, which is known if the lattice simulation is made. We however do not know the values: let us take some generic value between 0 and 1 as a guess: a half

$$|\langle P\rangle| = 1/2 = (1 - 2\cos(2\pi\delta))/3 \rightarrow \delta \approx 0.29. \tag{95}$$

If so, the fermion masses for the two sectors are $m/(2\pi T) = 0.29$ and 0.04, respectively. Such a large mass difference explains why the participation ratios (roughly, the fraction of the box volume occupied by a mode) are so different: while in the real sector the Dirac modes occupy only about 1% of the box, in the complex sectors nearly the whole box is occupied).

(v) Dirac eigenstates "at the gap"

The objects found via this method by Bruckmann *et al.* [26] are consistent with being made of L and $\bar{L}$ dyons. Apparently they must be neutral under the topological charge because they do not contribute to topological susceptibility. The clusters we propose in this work include both L and $\bar{L}$ dyons, with zero total topology, yet are still able to support the fermionic localized states. Further lattice studies of the Abelian-projected electric and magnetic fields correlated with those objects would further clarify their origins.

(vi) Dependence on fermionic periodicity conditions

In several works [20,23] the effects of the temporal boundary conditions on the chiral condensate on quenched ensembles was explored. In addition to the restoration of the chiral symmetry for the physical, *antiperiodic*, boundary conditions, an increase in the chiral condensate for the periodic condition above T_c was observed.

In the case of the adjoint fermions the drop of chiral condensate happens for both the periodic and antiperiodic sectors. There is however a qualitative difference: the drop is slower for the periodic case, differs in shape, and was not traced to reach zero. A qualitative difference is certainly expected on the basis of Ref. [32]: the zero modes for periodic and antiperiodic boundary conditions are drastically different. For the periodic case, all zero modes are democratically distributed, whereas for the antiperiodic boundary conditions they all fall onto the heaviest one (the L dyon). The case of antiperiodic boundary condition then restores chiral symmetry in the way similar to fundamental quarks, by condensation into $L\bar{L}$ clusters. The case of periodic adjoint fermions is quite different, it has a ''democratic'' distribution of zero modes over all dyons of the instanton. This makes restoration of the chiral symmetry much more difficult, as now correlating the ''heaviest'' $L\bar{L}$ is insufficient and also ''light'' $M\bar{M}$ pairs should form. A more quantitative analysis of the adjoint fermion case is reserved for future studies.

We finally comment that the case of dynamical adjoint fermions was treated analytically in [45], where it was shown that the chiral symmetry is indeed restored.

(vii) Short-range correlations of dyons in quenched and nonquenched ensembles

At high temperature, the vacuum is mostly dominated by perturbative fluctuations: the coupling is simply too small to allow for any kind of large quantum effects. As we lower the temperature, the formation of topological objects starts to be possible. Although still suppressed, the vacuum is able to polarize into topological objects, which can support localized fermionic modes of small eigenvalue, but still not small enough to break chiral symmetry. Also, the mass M of these zero modes, which interpolates from $2\pi T$ to πT i.e. reduces by half in units of temperature as temperature is decreased, makes it harder to break chiral symmetry at high temperature, as the tail of zero modes, being the inverse of this mass, does not extend very far, and, thus, at a small density of topological charge, the off-diagonal matrix elements are simply too small to matter, and the ensemble of dyons is the ensemble of $L\bar{L}$ pairs and neutral random clouds of light M, $\bar{M}$ dyons.

However things change drastically as temperature is decreased. The gluon dynamics facilitates the increase in topological density, due to a suppression of the action of any field configuration at lower temperature by the coupling $1/g^2$. At one point the moduli space metric of topological objects becomes the sole dictator of the distribution of the topological (dyonic) field configuration of the dyons, the rest simply being fluctuations, which is also not suppressed at all, but does not change the important topological properties of the background configuration. The dynamics of dyons becomes important solely through the geometry of the moduli space metric.

The interaction of L and anti-L is very similar to the interaction between L and L, i.e. they repel (Coulombic-like), and the L and anti-M attract from the point of view of the metric (at large distances), just like L and M. The vacuum then needs to undergo a transition in the structure, from pairs of $L\bar{L}$ and $M\bar{M}$, to the crystal of alternating dyons and antidyons.

Such an abrupt change in the vacuum structure of the quenched ensemble is absent upon introduction of dynamical fermions. In this case, the situation changes drastically. The increase in topological density is suppressed by the presence of fermions, as increasing density means making pairs come closer together. According to arguments in the article, such a scenario will make the fermionic determinant become smaller and smaller, eventually going to zero if the molecules overlap. That means that the same topological density is harder to develop with fermions. Increasing the flavors makes it even harder, as the smallness of the fermionic measure is enhanced by N_f. However, if N_f is not too large, chiral symmetry may still be broken, but the nature of this transition is now vastly different. The pairs try to keep their distance from all other pairs as large as possible.

(viii) Small comment about deconfiement

Recent work by Bruckmann *et al.* [46] argued that uncorrelated dyons of all kinds create linear confinement. We propose that an ensemble of correlated neutral molecules would not do that and generate short-range correlations only. This potentially links both deconfinement and chiral restoration with molecule formation.

ACKNOWLEDGMENTS

Strong motivation for this study during the last decade came from multiple discussions with P. van Baal. We also acknowledge more recent discussions with D. Diakonov and F. Bruckmann, as well as A G. Abanov. This work was supported in part by the US DOE under Grant No. DE-FG-88ER40388.

Note added—: After our paper was completed we learned of an important study [47] on the lattice, in which some of the tests proposed above were successfully performed. For *periodic* fermions, their near-zero eigenmodes with small eigenvalues are indeed identified with type-M,

$\bar{M}$ dyons, while for *antiperiodic* fermions those are indeed related with type-L, $\bar{L}$ dyons. This conclusion was reached by correlating the topology with the sign of the Polyakov line at the dyon center. The difference in inverse participation ratios between the two cases is indeed naturally explained by the large difference in M and L actions. For the "heavier" L dyons, even the shape of the fermionic eigenmodes was shown to agree with the corresponding semiclassical predictions.

APPENDIX: EXACT SOLUTION OF THE ZERO MODES

Although zero modes of a caloron were generally found elsewhere [10,11], here we use an approach that is more illuminating.

We solve Eqs. (32), where

$$\mathcal{H} = \pm\frac{1 - vr\coth(vr)}{r}, \tag{A1}$$

$$\mathcal{A} = \frac{1 - vr/\sinh(vr)}{r}. \tag{A2}$$

We will take the lower sign (anti–self-dual solution). To do this we separate the matrix $M(r)$ as

$$M(r) = M_0(r) + M_1(r), \tag{A3}$$

where

$$M_0(r) = \left(\frac{\mathcal{H}}{2} + \frac{1}{r}\right)1 = \frac{1 + rv\coth(rv)}{2r}, \tag{A4}$$

$$M_1(r) = \frac{z}{\beta}\sigma_1 + \left(\mathcal{A} - \frac{1}{r}\right)\sigma_3 = \frac{z}{\beta}\sigma_1 - \frac{v}{\sinh(vr)}\sigma_3. \tag{A5}$$

The solution can then be written as $\boldsymbol{\alpha} = \exp(-\int_0^r M_0(r)dr)\boldsymbol{\chi}$, or

$$\boldsymbol{\alpha} = \frac{1}{\sqrt{r\sinh rv}}\boldsymbol{\chi}. \tag{A6}$$

Note that if we took the upper sign in Eq. (A1), we would get a factor of $\sqrt{\sinh(vr)}$ in front of the solution. This is clearly non-normalizable, as it should be by the index theorem.

The differential equation for $\boldsymbol{\chi}$ is

$$\frac{d}{dr}\boldsymbol{\chi} = -M_1(r)\boldsymbol{\chi}, \tag{A7}$$

i.e.

$$\chi_1'(r) = \frac{v}{\sinh(vr)}\chi_1(r) - \frac{\phi}{\beta}\chi_2(r), \tag{A8}$$

$$\chi_2'(r) = -\frac{v}{\sinh(vr)}\chi_2(r) - \frac{\phi}{\beta}\chi_1(r). \tag{A9}$$

We may take a change of variables $\xi = rv$. Then the equations read

$$\chi_1'(\xi) = \frac{1}{\sinh(\xi)}\chi_1(r) - \mathfrak{s}\chi_2(r), \tag{A10}$$

$$\chi_2'(\xi) = -\frac{1}{\sinh(\xi)}\chi_2(r) - \mathfrak{s}\chi_1(r), \tag{A11}$$

where we labeled $\mathfrak{s} = \phi/(v\beta)$. We now eliminate ξ_2, and obtain the second order differential equation

$$-\frac{d^2}{d\xi^2}\chi_1 - \frac{1}{2\cosh^2\frac{\xi}{2}}\chi_1 = -\mathfrak{s}^2\chi_1. \tag{A12}$$

This equation has a general solution

$$\chi_1(\xi) = c_1\left(-2\mathfrak{s} + \tanh\frac{\xi}{2}\right)e^{\mathfrak{s}\xi} + c_2\left(2\mathfrak{s} + \tanh\frac{\xi}{2}\right)e^{-\mathfrak{s}\xi} \tag{A13}$$

with arbitrary constants $c_{1,2}$. Using the first order equations. we can write χ_2 as

$$\chi_2(\xi) = c_1\left(2\mathfrak{s} - \coth\frac{\xi}{2}\right)e^{\mathfrak{s}\xi} + c_2\left(2\mathfrak{s} + \coth\frac{\xi}{2}\right)e^{-\mathfrak{s}\xi} \tag{A14}$$

The function $\chi_2(\xi)$ is divergent when $\xi \to 0$, except if $c_1 = c_2$, in which case $\xi_2(0) = 0$. Therefore, $c_2 = c_1$. The constant c_1 can be determined by the overall normalization. The solution then becomes

$$\chi_1(\xi) = 2c_1\left(-2\mathfrak{s}\sinh(\xi\mathfrak{s}) + \tanh\frac{\xi}{2}\cosh(\xi\mathfrak{s})\right) \tag{A15a}$$

$$\chi_2(\xi) = 2c_1\left(2\mathfrak{s}\cosh(\xi\mathfrak{s}) - \coth\frac{\xi}{2}\sinh(\xi\mathfrak{s})\right). \tag{A15b}$$

Finally, combining with (A6) we obtain

$$\alpha_{1,2} = \frac{\sqrt{v}}{\sqrt{\xi\sinh\xi}}\chi_{1,2}. \tag{A16}$$

$\sqrt{v}$ can be absorbed into constant c_1, and our final expression is

$$\alpha_{1,2} = \frac{\chi_{1,2}}{\sqrt{\xi\sinh\xi}}, \tag{A17}$$

with functions $\chi_{1,2}$ given by (A6), $\xi = vr$, $\mathfrak{s} = \phi/(v\beta)$. Note that the value of $\alpha_1(\xi \to 0)$ is given by

$$c_1(1\text{–}4\mathfrak{s}^2), \tag{A18}$$

and the solution is completely regular at $r = 0$. Remarkably it turns out that for $c_1 = 1/2$, the solution is already normalized (in the sense of $\int d\xi\xi^2$ integration).

[1] F. Bruckmann, D. Nogradi, and P. van Baal, Acta Phys. Pol. B **34**, 5717 (2003).
[2] D. Diakonov, Nucl. Phys. B, Proc. Suppl. **195**, 5 (2009).
[3] E. M. Ilgenfritz and E. V. Shuryak, Nucl. Phys. **B319**, 511 (1989).
[4] D. Diakonov, N. Gromov, V. Petrov, and S. Slizovskiy, Phys. Rev. D **70**, 036003 (2004).
[5] J. Liao and E. Shuryak, Phys. Rev. C **75**, 054907 (2007).
[6] E. V. Shuryak, arXiv:hep-ph/9909458.
[7] E. Poppitz and M. Unsal, J. High Energy Phys. 07 (2011) 082.
[8] T. Schafer and E. V. Shuryak, Rev. Mod. Phys. **70**, 323 (1998).
[9] A. A. Belavin, A. M. Polyakov, A. S. Schwartz, and Yu. S. Tyupkin, Phys. Lett. **59B**, 85 (1975).
[10] K.-M. Lee and C.-h. Lu, Phys. Rev. D **58**, 025011 (1998).
[11] T. C. Kraan and P. van Baal, Phys. Lett. B **435**, 389 (1998).
[12] M. Unsal, Phys. Rev. D **80**, 065001 (2009).
[13] K. Miura, M. P. Lombardo, and E. Pallante, Phys. Lett. B **710**, 676 (2012).
[14] A. Deuzeman, M. P. Lombardo, and E. Pallante, arXiv:1012.6023.
[15] A. Cheng, A. Hasenfratz, and D. Schaich, Phys. Rev. D **85**, 094509 (2012).
[16] G. Cossu, M. D'Elia, A. Di Giacomo, G. Lacagnina, and C. Pica, Phys. Rev. D **77**, 074506 (2008).
[17] R. D. Mawhinney, Nucl. Phys. B, Proc. Suppl. **83**, 57 (2000).
[18] X. Y. Jin and R. D. Mawhinney, Proc. Sci., LAT2009 (2009) 049 [arXiv:0910.3216].
[19] F. Bruckmann, D. Nogradi, and P. van Baal, Nucl. Phys. **B666**, 197 (2003).
[20] E. Bilgici, F. Bruckmann, J. Danzer, C. Gattringer, C. Hagen, E. M. Ilgenfritz, and A. Maas, Few-Body Syst. **47**, 125 (2010).
[21] C. Gattringer, M. Gockeler, P. E. L. Rakow, A. Schafer, W. Soldner, and T. Wettig, Nucl. Phys. B, Proc. Suppl. **106**, 492 (2002).
[22] F. Bruckmann, Proc. Sci., CONFINEMENT8 (2008) 179 [arXiv:0901.0987].
[23] E. Bilgici, C. Gattringer, E.-M. Ilgenfritz, and A. Maas, J. High Energy Phys. 11 (2009) 035.
[24] C. Gattringer and S. Schaefer, Nucl. Phys. **B654**, 30 (2003).
[25] C. Gattringer, Phys. Rev. Lett. **88**, 221601 (2002).
[26] F. Bruckmann, T. G. Kovacs, and S. Schierenberg, Phys. Rev. D **84**, 034505 (2011).
[27] K. M. Lee and P. Yi, Phys. Rev. D **56**, 3711 (1997).
[28] N. S. Manton, Nucl. Phys. **B126**, 525 (1977).
[29] J. N. Goldberg, P. S. Jang, S. Y. Park, and K. C. Wali, Phys. Rev. D **18**, 542 (1978).
[30] S. F. Magruder, Phys. Rev. D **17**, 3257 (1978).
[31] E. Poppitz and M. Unsal, J. High Energy Phys. 03 (2009) 027.
[32] M. Garcia Perez, A. Gonzalez-Arroyo, and A. Sastre, J. High Energy Phys. 06 (2009) 065.
[33] For the explicit form of function $\mathcal{H}$, $\mathcal{A}$, see the Appendix.
[34] This ansatz is inspired by the fact that the fermions have two $SU(2)$ indices, one spin and one color. Since we consider the fundamental color representation (i.e. both are **2** representations), these indices can be combined into $\mathbf{2} \otimes \mathbf{2} = \mathbf{0} + \mathbf{3}$, which is precisely the decomposition considered in the text.
[35] R. Jackiw and C. Rebb, Phys. Rev. D **13**, 3398 (1976).
[36] S. Gabor, *Orthogonal Polynomials* (American Mathematical Society, Providence, RI, 1995).
[37] E. V. Shuryak, Zh. Eksp. Teor. Fiz. **74**, 408 (1978) [Sov. Phys. JETP **47**, 212 (1978)].
[38] In 1977, when QCD was only 4 years old, the main finding was its positivity, which ensured *screening* of a charge, as opposed to antiscreening by vacuum loops: thus the name "plasma."
[39] R. D. Pisarski and L. G. Yaffe, Phys. Lett. **97B**, 110 (1980).
[40] E. V. Shuryak, Nucl. Phys. **B203**, 140 (1982).
[41] Note that the explicit numerical factors and the definition of the Λ parameter are not really important since they will change in a theory with fermions.
[42] We also ignored the small nondiagonal matrix elements of the type $m\langle I_1|I_2\rangle$ resulting from the nonorthogonality of the zero modes of different pseudoparticles.
[43] K.-Y. Kim, S.-J. Sin, and I. Zahed, J. High Energy Phys. 09 (2008) 001.
[44] This dip should not be confused with that due to the finite size of the system, which is well described by the random matrix theory.
[45] M. Unsal, Phys. Rev. Lett. **100**, 032005 (2008).
[46] F. Bruckmann, S. Dinter, E. M. Ilgenfritz, B. Maier, M. Muller-Preussker, and M. Wagner, Phys. Rev. D **85**, 034502 (2012).
[47] V. G. Bornyakov, E.-M. Ilgenfritz, B. V. Martemyanov, and M. Muller-Preussker, Phys. Rev. D **79**, 034506 (2009).